2021

CONTROLS ON NO3-N DYNAMICS IN THE UPPER CLARK FORK RIVER, MONTANA

Jacob Anthony Prater

CONTROLS ON NO_3-N DYNAMICS IN THE UPPER CLARK FORK RIVER, MONTANA

By

JACOB ANTHONY KEKOA PRATER

Bachelor of Arts, Seattle University, Seattle, Washington, 2019

Thesis

Presented in partial fulfillment of the requirements

for the degree of

Master of Science

In Systems Ecology

The University of Montana

Missoula, Montana

May 2021

Dr. H. Maurice Valett, chair

Division of Biological Sciences, University of Montana

Dr. Robert O. Hall, committee member

Flathead Biological Station

Dr. Matthew J. Church, committee member

Flathead Biological Station

Dr. Michael D. DeGrandpre, committee member

Department of Chemistry and Biochemistry, University of Montana

Acknowledgements

I thank Sophie Buckland and Nicholas Carpenter for their field support and friendship, as well as Claire Utzman and Kimberly Bray for their imperative contributions in the laboratory. I would like to thank all members of the Valett Aquatic Ecosystem Ecology Laboratory for the many hours of productive conversation leading to the ideas presented here, including Colton Kyro, Taylor Gold-Quiros, and Dr. Rafael Feijo de Lima. I would like to express my gratitude to my supervisor Dr. H. M. Valett for the trust he put in me, as well as the unwavering support and guidance he provided throughout my graduate career. Lastly, I thank my family for their continued support and encouragement throughout the entirety of my undergraduate and graduate career. This work was supported by the National Science Foundation EPSCoR Cooperative Agreement OIA-1757351.

CONTROLS ON NO_3-N DYNAMICS IN THE UPPER CLARK FORK RIVER, MONTANA

Chairperson: Dr. H.M. Valett

Studies relating ecosystem energetics to nutrient uptake in streams have generally found respiration to be a more dominant control on nutrient dynamics relative to primary production due to light limitation in most low-order systems. In this study, I measured biomass, hydrology, metabolism, and dissolved solutes in an open-canopy mid-order river located in western MT. Daily stream metabolism was modeled using a modified single-station, open-channel method, and measures of dissolved solutes were evaluated at both local and reach scales to examine how point-measures and those integrated through space represent biogeochemical behavior. Metabolic rates and standing stocks of benthic organic matter were greater at Site 2 despite greater nutrients loads delivered to Site 1. Benthic organic matter ranged from 1.11-60.4 g OM m^{-2} and chlorophyll *a* from 40.9-150.9 mg Chl a m^{-2} between sites. GPP ranged from 1.89 to 11.14 g O_2 m^{-2} and ER from -0.93 to -8.66 g O_2 m^{-2} d^{-1} with greater rates observed at Site 2. The fraction of GPP consumed as autotrophic respiration (AR_f) was high at both sites, 76 and 66% for Sites 1 and 2, respectively. Mean loads for NO_3-N at Site 1 (61.29 ± 4.92 kg N d^{-1}) were greater than loads delivered to Site 2 (27.02 ± 3.36 kg N d^{-1}), and an effective solute flux (U_{eff}) calculated from mass-balance that the reach between sites is a biological sink for NO_3-N. Compared to hydrologic losses, biological uptake ($U_{eff\text{-}bio}$) accounted for nearly 90% of the reduction in material loads. Correlation between $U_{eff\text{-}bio\text{-}NO3}$ and NEP ($r^2 = 0.22$, $p < 0.01$), as well as calculated autotrophic N demand (U_{dem}) derived from NPP ($r^2 = 0.29$, $p < 0.01$), suggests that autotrophic assimilation is a major control on changes in material load. Average U_{dem} (147.7 ± 6.06 mg N m^{-2} d^{-1}), however, was nearly triple the mean value for $U_{eff\text{-}bio\text{-}NO3}$, suggesting unmeasured sources of DIN linked to autotrophic assimilation via other processes such as N-fixation, nitrification, and N mineralization.

Introduction

Anthropogenic eutrophication and associated biological and chemical alterations to inland waters is well documented (Smith et al. 1999, Dodds and Smith 2016). In the context of nitrogen (N) loads to downstream reaches, small streams (Peterson et al. 2001) and large rivers (Tank et al. 2008) act as active processing sites with the potential to transform and retain dissolved nutrients. Since the spiraling concept (Newbold et al. 1981) provided a framework for integrating transport and uptake of nutrients in streams, others have demonstrated the influence that in-stream processing can have on material loads and how biogeochemical function may differ within (Mulholland et al. 1995, Jones et al. 2018) and among (Webster et al. 2003, Mulholland et al. 2009, Hall et al. 2013) river systems. Moreover, recent work has recognized a central role for ecosystem stream metabolism as a determinant of lotic nutrient cycling and material retention (Mulholland et al. 2001, Heffernan and Cohen 2010).

In Grand Teton National Park, gross primary production (GPP) and ecosystem respiration (ER) explained 82% of variation in the uptake velocity (V_f) of ammonium (NH_4^+), while GPP alone explained variation in nitrate (NO_3^-) V_f (Hall and Tank 2003a). Stemming from a dataset collected as part of the Lotic Intersite Nitrogen eXperiment (LINX) project, NH_4^+ uptake (U) and V_f were correlated with ER across 11 systems ranging from the North Slope of Alaska to Puerto Rico (Webster et al. 2003). Others have synthesized studies relating nutrient spiraling metrics to ecosystem metabolism, and have generally found the uptake of dissolved solutes to be more generally controlled by CR, rather than GPP (Hoellein et al. 2007). However, in well-lit, warm systems, autotrophs and their associated rates of carbon fixation may act as a more dominant control on nutrient dynamics. GPP was negatively correlated to day-to-day changes in nocturnal NO_3^- concentration maxima in the spring-fed Ichetucknee River, Florida, where heterotrophic

assimilation was minimal (Heffernan and Cohen 2010). Additionally, (Jones et al. 2018) reported that NO_3^- retention over a 16-km reach of Clear Creek, IA, a fourth-order stream draining an agricultural watershed, was tied to autotrophic assimilation by relating downstream reductions in NO_3^- concentration to O_2 production.

The Upper Clark Fork River (UCFR) of western Montana, a mid-order river characterized by warm, well-lit water for much of the growing season, displays seasonal proliferation of benthic algae with standing crops comparable to those reported for renowned smaller streams fueled by autotrophy like Deep Creek (Minshall et al. 1978) and Sycamore Creek (Busch and Fisher 1981). As a productive mid-order river the UCFR is an excellent system in which to relate nutrient dynamics to metabolism with the intention to examine primary production as a dominate control. Relatively little is known about rates of metabolism in the UCFR; A single study addressing the Middle Clark Fork River estimated net ecosystem production (NEP) at one location downstream where the river is much larger, identified periods of autotrophic behavior (Lynch et al. 2010). To address the potential for autotrophic control over N retention, I coupled measures of ecosystem metabolism derived from whole-system approaches to nutrient uptake rates generated by a mass-balance approach. As foci for the research, I addressed two central questions: (1) How do NO_3^- dynamics and ecosystem metabolism differ between two sites along a 20km flow path? And (2) along the river segment linking the two sites, what combination of biological and physical mechanisms account for reach behavior and help explain observed differences in the biogeochemical and metabolic regimes observed at the two Sites?

Methods

Site description

I conducted this study on the UCFR, MT, which drains a 57,000 km^2 watershed as an open-channel, snow-melt driven river. The river originates at the confluence of Silver Bow Creek and Warm Springs Creek (Figure 1). Discharge in the UCFR near Deer Lodge, MT is generally highest from May-June (25 – 30 m^3/s), returning to baseflow during July-August (4-6 m^3/s). I established two sites that were approximately 20 river km apart, with the upstream site (Site 1, 46.3826°N, -112. 7328°W) located at Arrow Stone Park in Deer Lodge, MT, and the downstream site (Site 2, 46.4979°N, -112.7409°W) at a public fishing access site near Garrison, MT (Figure 1). Between the two sites, the river is well-lit, with an open channel, flowing primarily through an agricultural landscape supporting hay and cattle production with much of the riparian corridor characterized by grasses, shrubs and relatively sparse tree cover (Lejeune et al. 1996). Remediation activities have taken place for decades to mitigate metal influences on the river's floodplain resulting from 19^{th} and 20^{th} century mining of heavy metals in the Butte-Silver Bow Creek area of southwest Montana (Neuman et al. 2008). However, rising stream water temperatures, lower flows, and increases in nutrient availability provide compounding influences on productivity and resilience of biological communities along the UCFR (Stagliano 2020).

Physical and Physicochemical Properties

Daily discharge (Q, m^3/s) at each site was obtained by establishing relationships between measured stream flow using an acoustic Doppler current profiler (ADCP, StreamPro, RD

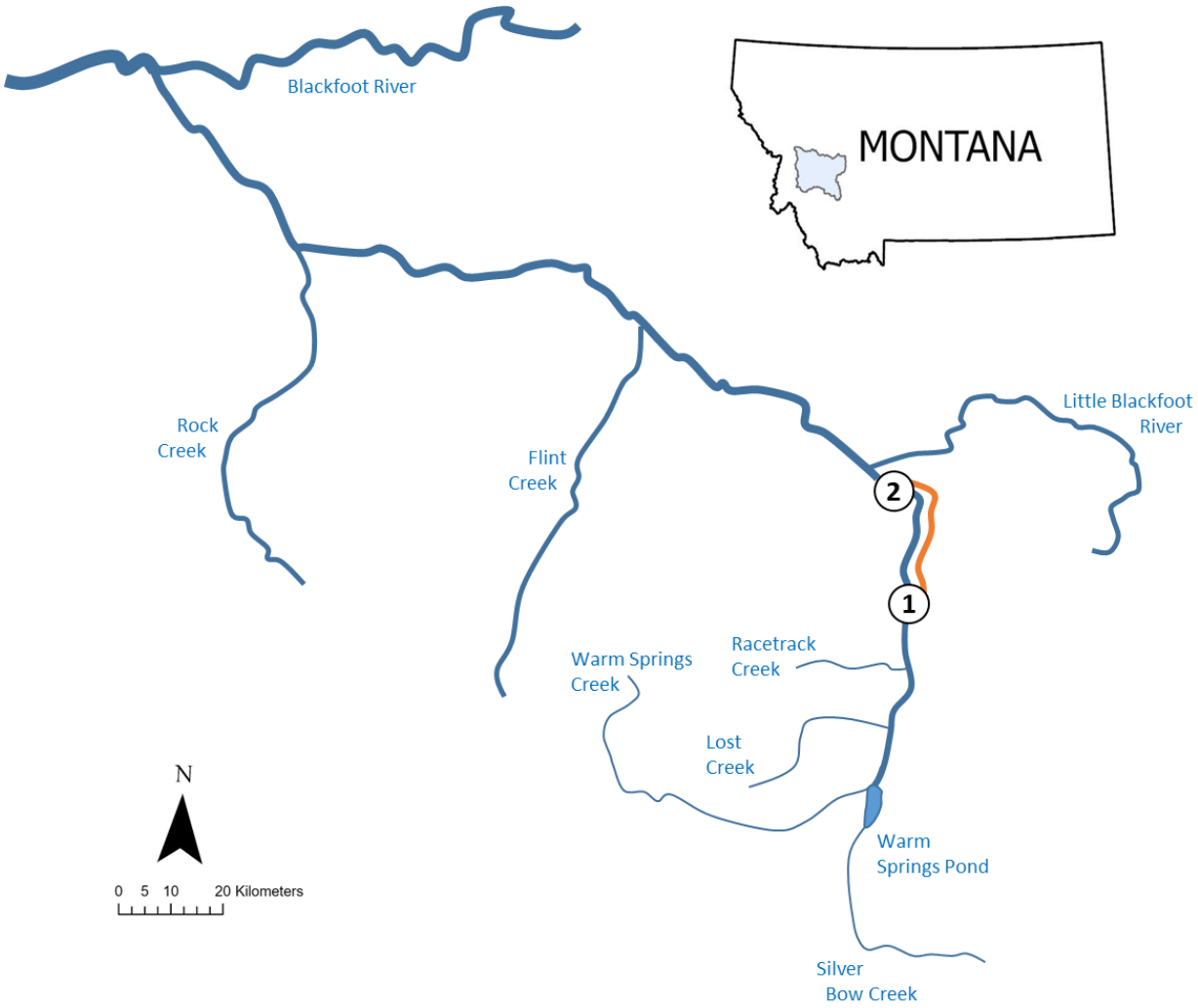

Figure 1: Study sites and major tributaries along the UCFR including Site 1 (upstream) and Site 2 (downstream). Orange line indicates the 20-km reach between sites.

Instruments, Poway, CA) and Q measurements available from near-by USGS monitoring stations (USGS 12324200 Clark Fork at Deer Lodge MT and USGS 12324400 Clark Fork above Little Blackfoot R near Garrison MT, $r^2 = 0.98$, $p < 0.001$ and $r^2 = 0.99$, $p < 0.001$ for Sites 1 and 2, respectively). At each site, specific electrical conductivity (Spc, µS/cm), temperature (°C), dissolved oxygen (DO, mg/L), and DO saturation (DO_{sat}, %) were monitored using in situ sensors beginning in mid-July (July 13th, 2020) at the recession of peak flow and ending in mid-October (October 19, 2020) at the conclusion of the growing season. Stream water Spc (Onset HOBO Conductivity Logger, Bourne, MA), temperature, DO and DO_{sat} (PME miniDOT, Vista, CA) were recorded at 10-minute intervals using sensors deployed at 0.5 depth at each site. Sensor maintenance and cleaning was performed 2 to 3 times weekly.

Water Chemistry

Water chemistry was measured two to three times weekly from July 13, 2020 through October 19, 2020. Water samples (n=3) were collected at each site using HDPE bottles, and filtered in the field (Whatman GF/F, 0.7 µm-pore size) into polypropylene tubes for nutrient analysis. Samples were stored on ice for transport to laboratory, where they were frozen (-20°C) until analysis.

Filtered water samples were analyzed for N as nitrate-nitrite (reported as NO_3-N, mg/L) and ammonium-N (NH_4-N, mg/L), and for P as soluble reactive phosphorus (SRP, mg/L) using a Segmented Flow Analyzer (Astoria-Pacific AP2, Clackamas, OR). Analysis of NO_3-N was performed using cadmium-reduction chemistry (O`Dell 1993a) and $NH_4$-N analyses according to the phenol-hypochlorite colorimetry method (O`Dell 1993b). SRP concentrations were determined using the ascorbic acid colorimetry method (O`Dell 1993c). Dissolved inorganic nitrogen (DIN) was calculated as the sum of NO_3-N and NH_4-N.

Biomass

I sampled benthic standing crops weekly at both sites from July 13, 2020 – October 19, 2020 except for the week of October 12th, where I only sampled Site 1 due to heavy wind and snow. I collected benthic biomass by placing a metal, cylindrical benthic sampler (area = 0.26 m^{-2}) directly on the stream bottom and recording four cardinal depths within the sampler. I collected all coarse organic material, mostly filamentous algae, from all consolidated substrate (i.e., cobbles, pebbles) and stored in polyethylene bags. Substrate surfaces were then scrubbed using a wire brush and a spray bottle to remove all epilithic material which was then added to the collected samples. Samples were transported to lab in a cold, dark cooler, and placed in dark, cold-storage until processing, generally within 24 hours.

I measured benthic organic matter (BOM) standing stocks (g/m^2) as Ash-Free Dry Mass (AFDM), and I estimated the abundance of primary producers as chlorophyll-*a* standing crops (Chl a, mg/m^2). I processed epilithic material in lab for AFDM by recording a sample's total volume, and vacuum filtering a sub-sample of known volume. Weights of filters were recorded following a 24-hour drying period at 60ºC to represent dry mass. Filters were subsequently ashed for 1 hour at 550 ºC, cooled, and re-weighed to determine ash mass. I calculated AFDM was the difference between dry mass and ash mass. Filamentous samples were processed for AFDM by recording a wet weight, then drying and ashing at the same temperatures previously described. Total BOM standing stock (epilithon and filamentous) was then calculated based on the sub-sample:total volume ratio and the area of the benthic sampler.

Epilithon was processed for Chl a by recording a total volume, and vacuum filtering a known volume. I distributed filters and all material retained on them into polypropylene tubes with 10 mL of 90% buffered acetone for pigment extraction. Filamentous samples were processed by

recording an initial wet weight and extracting 0.5 g subsample in 90% buffered acetone (Şükran et al. 1998). Following centrifugation, a 3-ml sample was transferred from each falcon tube to a quartz cuvette, and analyzed for Chl a following Ritchie (2008). Final standing crops were calculated including corrections for sub-sampling and normalized to sampling area.

Metabolism

Daily metabolism was estimated from July 22 to October 19, 2020 at Site 1, and July 13 to October 19, 2020 at Site 2 using a modified version of the single-station open-channel method (Odum 1956, Hall and Hotchkiss 2017), which employs modeled photosynthetic photon flux density, depth (m), DO, and water temperature to derive metabolic parameters (*streamMetabolizer* package version 0.10.9, Appling et al. 2018). Data for temperature and DO were derived from in-stream sensors, and depth was obtained by creating a regression between average reach depth measurements and discharge (n=4) for the reaches upstream of Site 1 (r^2 = 0.81, p = 0.06) and 2 (r^2 = 0.77, p = 0.07). Parameters for daily gross primary productivity (GPP, g $O_2/m^2/d$), daily ER (g $O_2/m^2/d$) and the oxygen gas-exchange coefficient normalized to Schmidt number of 600 (K_{600}, d^{-1}) were estimated using the R package *streammetabolizer* (Appling et al. 2018). Values for K_{600} were used to assess the validity of metabolic parameter estimations by examining possible relationships between gas exchange and ER (Figure S1). Following metabolic estimates, two daily gaps in ER were interpolated using the R packages *zoo* (R version 1.8.8) and *dplyr* (R version 1.0.2). To fill gaps in data, I created a data frame of the metabolic estimates, read the data frame as a zoo product, and used linear interpolation.

To estimate the fraction of GPP consumed by autotrophic respiration (AR_f), I used a quantile regression approach as employed by Hall and Beaulieu (2013). Operationally, autotrophic respiration (AR) corresponds to the upper limit of the relationship between ER and GPP (where

ER is negative), as it represents respiratory activity of organisms responsible for GPP itself. Quantile regression was used to quantify the relationship between the upper quantile of ER vs GPP, given that quantile regression estimates quantiles of y conditioned on x (Koenker and Hallock 2001, Cade and Noon 2003). The 0.9 quantile is chosen as a tradeoff between describing the upper edge of the data and having sufficient data for accurate quantification (Hall and Beaulieu 2013). The slope of the 0.9 quantile of the relationship between ER and GPP is representative of the percentage of GPP respired as AR. All quantile regressions were performed in R Studio (version 3.6.1) using the R package *quantreg* (R version 5.75).

Rates of net ecosystem production (NEP, $g/m^2/d$) were derived as the sum of GPP and ER and converted to C units assuming a respiratory quotient of 0.85 (Bott et. al. 1979). Net primary production (NPP, $g\ O_2/m^2/d$) was derived by summing estimates of AR and GPP. Putative metabolic demand for N or P (U_{dem}, $mg/m^2/d$) was derived from NPP by first converting rates of NPP to rates of C (CO_2) fixed using a photosynthetic quotient of 1.2 (Wetzel and Likens 2000, Webster et al. 2003). Rates of C fixed were then converted to $U_{dem\text{-}N}$ using a molar C:N ratio of 6.625, or to $U_{dem\text{-}P}$ using a C:P ratio of 106 following Redfield (1934).

Local and reach scale nutrient dynamics

To assess local and reach-scale nutrient dynamics, instantaneous measures of load (L, kg/d) and net changes in load (ΔL, kg/d) were quantified over the growing season using concentration (C, mg/L as N or P), and an average Q centered around sampling events. Changes in Q (ΔQ, m^3/s) were calculated from differences in stream flow between Site 1 to Site 2. Material loads were calculated for each sampling event following equation (1):

$$L = C \times Q \times 86.4 \quad (1)$$

where 86.4 is a constant used to convert units. Site-specific measures of effective first-order longitudinal uptake rates (k_{eff}, km^{-1}) were derived from estimates of U_{dem}, reach width (w, m), nutrient load (mg/d) and a conversion factor via equation (2):

$$k_{eff} = \frac{U_{dem}}{L} \times w \times 10^3 \quad (2)$$

Change in material load over the reach extending from Site 1 to Site 2 (ΔL, kg/d) was derived by subtracting downstream loads (L_{down}) from upstream loads (L_{up}) following equation (3):

$$\Delta L = L_{down} - L_{up} \quad (3)$$

Hence, positive ΔL values indicate net accumulation of the material of interest, and negative ΔL values indicate net load reduction. Under conditions when river flow declined from Site 1 to Site 2, change in loads attributed to hydrologic loss (ΔL_{hydro}) were calculated using ΔQ and a geometric mean (GM) of solute concentrations at Sites 1 and 2 (C_{up}, C_{down}) via to equation (4):

$$\Delta L_{hydro} = \Delta Q \times GM\left(C_{up}, C_{down}\right) \times 86.4 \quad (4)$$

The influence of ΔL_{hydro} on ΔL could not be estimated when ΔQ was positive due to lack of representative values for concentration of solutes in sources contributing to increased hydrologic load. Change in loads attributed to biogeochemical processes (ΔL_{bio}) were calculated by subtracting ΔL_{hydro} from ΔL (Eq 5):

$$\Delta L_{bio} = \Delta L - \Delta L_{hydro} \quad (5)$$

Net changes in load were also expressed as effective solute flux (U_{eff}, $mg/m^2/d$), a solute flux attributed to hydrologic loss ($U_{eff\text{-}hydro}$, $mg/m^2/d$) and to biogeochemical processes ($U_{eff\text{-}bio}$, $mg/m^2/d$) using their respective ΔL variable normalized to streambed area (A, m^2). Reach area was determined as the product of reach length (m) and channel width (w, m), derived from regression relationships with Q measures based on calibration data at each of the USGS gauges.

To create a proportional reach-scale assessment of biogeochemical function to compare to those derived for point-measures, I calculated an effective longitudinal uptake rate attributed to biology ($k_{reach\text{-}bio}$) following equation (6):

$$k_{reach-bio} = \frac{U_{eff-bio}}{GM(L_{up}, L_{down})} \times w \quad (6)$$

where GM (L_{up}, L_{down}) is the geometric mean for material loads derived from upstream and downstream sites. A full list of terms can be found in the supplementary information (Table S1).

Statistical Analyses

Differences between means were assessed using paired t-tests and Welch's t-tests. One sample t-tests for location were used to compare the values of certain variable to criterion measures (i.e., P:R = 1, NEP = 0). Changes over the growing season for individual variables, and relationships between monitored variables, were analyzed via linear regression. Variables that displayed temporal autocorrelation were analyzed using univariate generalized additive models (GAM) with restricted maximum likelihood smoothness selection (REML) using the *mgcv* package (R version 1.8.28, Simpson 2018) in order to accurately assess changes in variables through time. In cases where a GAM with REML displayed persistent residual autocorrelation, a continuous first-order (CAR(1)) autoregressive process was added to the model (Simpson 2018), and best fit models of each time series were assessed using Akaike information criterion. Periods of change in each modeled time series were identified by points at which the 95% simultaneous confidence interval of the first derivative did not include zero. First derivatives were calculated using the *gratia* package (R version 0.5.0). To assess relationships between autotrophic metabolic activity (available for individual sites) and reach biogeochemical uptake (i.e., $U_{eff\text{-}bio}$), I employed a reach-scale metabolic measure using a weighted value for NPP. Values used as weights for the two site measurements were determined using progressive combinations of

weighted values and best fit assessed via respective p-values and coefficients of determination (R^2). Associated values for $U_{dem\text{-}N}$ were then derived from weighted values of NPP to address the relative magnitudes of calculated autotrophic demand and empirical reach-scale measures of N uptake.

Results

Physicochemical conditions

During sampling from July to October, river flow at the two sites declined from maxima near 17 m^3/s in June to minimal flows near 4-5 m^3/s during August. Stream temperatures at Site 1 (4.6 – 21.5 °C) were similar to those at Site 2 (4.5 – 20.0 °C, $p > 0.05$) with mean values differing by only 0.4°C (Table 1). Specific electrical conductivity, a general measure of ionic strength, was similar between sites (367.5 ± 0.38 versus 359.8 ± 0.30 µS/cm, respectively, Table 1, $p > 0.05$). Limits for DO (~7-10 mg/L) and DO_{sat} (~75-95%) within sites. Mean DO ($p < 0.05$) and DO_{sat} ($p < 0.001$) at Site 2 exceeded those at Site 1 by 0.24 mg/L and 3.1% DO_{sat}, respectively (Table 1).

Dissolved nutrient availability differed between sites, with mean NH_4-N concentration at Site 1 (0.015 ± 0.001 mg/L) more than double that at Site 2 (0.007 ± 0.0006 mg/L, Table 1, $p < 0.001$). Similarly, mean NO_3-N concentration was more than two-fold greater at Site 1 (0.099 ± 0.006 Table 1, $p < 0.001$) relative to Site 2 (0.042 ± 0.006 mg/L). Maximal values of NO_3-N were similar between sites (0.16 vs 0.14 for Sites 1 and 2), but minimum values at Site 2 (as low as 0.001 mg/L) were much lower than those observed at Site 1 (0.022 mg/L, Figure S2). Neither site exhibited an extended temporal trend in NO_3-N concentration over the growing season ($r^2_{adj} = 0.564$, *edf* = 3.515, n = 30; $r^2_{adj} = 0.838$, *edf* = 6.272, n = 30, Figure S2) despite apparent increases in concentration during later stages of monitoring. Across measures of NO_3-N and

Table 1: Longitudinal differences in physicochemical and chemical characteristics between sites. Values are grand means (lower 95% confidence limit, upper 95% confidence limit, n) based on biweekly sampling. P values reflect results from either paired or Welch's two-sample t tests to assess differences between sites and are indicated as: ns, $p > 0.05$; *, $p < 0.05$; **, $p < 0.01$; ***, $p < 0.001$ following t-tests for location.

	Site 1	Site 2	P
Q (m^3 s^{-1})	8.24 (7.54, 8.95, 104)	8.62 (7.63, 9.62, 104)	*ns*
Temperature (°C)	14.1 (13.2, 14.9, 92)	14.5 (13.7, 15.3, 98)	*ns*
Specific Conductance (µS cm^{-1})	367.5 (361.0, 374.0, 73)	359.8 (354.0, 365.6, 89)	*ns*
DO (mg L^{-1})	8.65 (8.50, 8.80, 92)	8.89 (8.73, 9.04, 98)	*
DO (%)	83.8 (83.1, 84.4, 92)	86.9 (86.2, 87.6, 98)	***
NH_4-N (mg L^{-1})	0.015 (0.013, 0.017, 30)	0.007 (0.006, 0.008, 30)	***
NO_3-N (mg L^{-1})	0.099 (0.08, 0.11, 30)	0.042 (0.02, 0.05, 30)	***
DIN (mg L^{-1})	0.11 (0.09, 0.12, 30)	0.05 (0.03, 0.06, 30)	***
SRP (mg L^{-1})	0.030 (0.0, 0.06, 30)	0.024 (0.018, 0.030, 30)	*ns*
Molar N:P	120.3 (65.1, 175.6, 26)	14.6 (6.14, 23.1, 30)	***

NH_4-N, NO_3-N accounting for 90 and 84% of DIN composition at Sites 1 and 2, respectively. In contrast to differential N availability, SRP was abundant at both sites and the mean concentration observed at Site 1 (0.030 ± 0.018 mg/L) was similar to that measured at Site 2 (0.024 ± 0.002 mg/L, $p > 0.05$, Table 1). Given the distribution of inorganic N and P constituents, the molar N:P ratio was substantially greater at Site 1 (120.3 ± 26.8) compared to Site 2 (14.6 ± 4.15, $p < 0.001$, Table 1).

Biomass

Both BOM (11.1 ± 1.77 g/m^2) and Chl a *(*40.9 ± 9.88 mg/m^2) were lower at Site 1 when compared to downstream standing crops (60.4 ± 9.08 g OM/m^2 and 150.9 ± 9.75 mg Chl a/m^2, respectively, $p < 0.001$, Figure 2a,b). During the first 21 days of monitoring, BOM standing stocks at Site 2 were 3-4-fold greater than those at the upstream site. Across all dates, however, directional decline in BOM at Site 2 ($r^2 = 0.65$, $p < 0.001$) resulted in lower and similar standing stocks late in the growing season (9.99 ± 082 and 14.1 ± 0.42 g OM/m^2 for Sites 1 and 2, respectively, Figure 2a). Similarly, Chl a at Site 2 declined with time ($r^2 = 0.34$, $p < 0.01$, Figure 2b) to approximately 50% of early season abundances. In contrast, neither BOM nor Chl a displayed distinct temporal trends over the growing season at Site 1 (Figure 2a,b). In combination, changes in BOM and Chl a at Site 2 resulted in a significant change in BOM composition as Chl a:BOM ratio increased directionally ($r^2 = 0.58$, $p < 0.01$) from a minimum of 0.001 to a maximum of 0.007 (Figure 2c). Over the same time course, relative abundance of Chl a at Site 1 varied, did not change directionally with time ($p > 0.05$, Figure 2c), and resulted in a mean Chl a*:*BOM value of 0.003 ± 0.003 (Figure 2c).

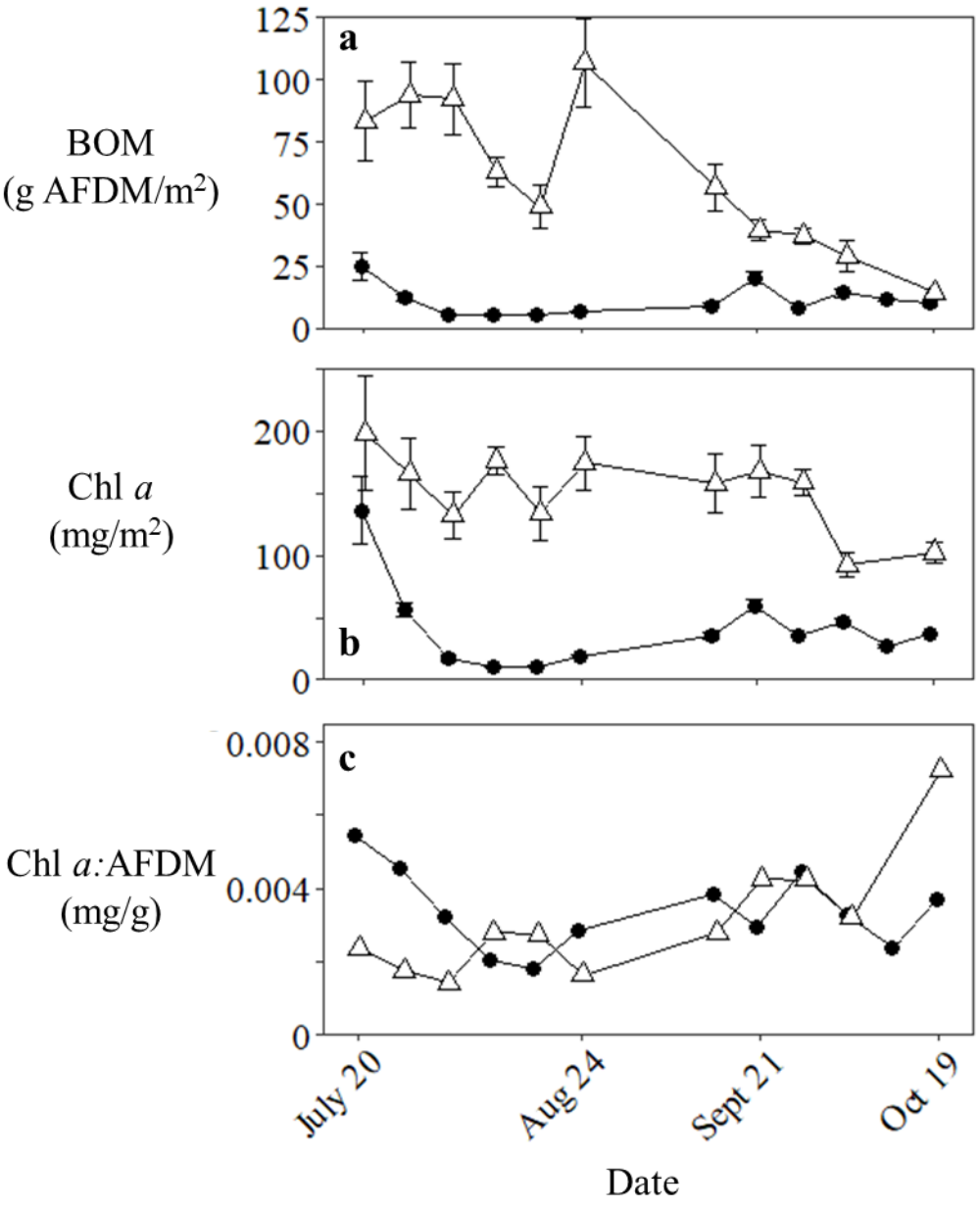

Figure 2: Time course for (a) BOM (g AFDM/m^2) and (b) Chl a (mg/m^2) at Site 1 (filled circles) and Site 2 (open triangles). Data are means ± standard errors.

Spatial Differences in Metabolic Regime

Rates of ecosystem metabolism differed between the two sites, broadly reflecting greater downstream metabolic activity. Between the two sites, GPP ranged from 1.9 to 11.1 g $O_2/m^2/d$ (Figure 3a,b), with the magnitude of primary production greater ($p < 0.001$) downstream (6.3 ± 0.2 g $O_2/m^2/d$) than upstream (4.5 ± 0.1 g $O_2/m^2/d$). A similar relationship was displayed for ER, which varied from -0.9 to -8.7 g $O_2/m^2/d$ within the two sites (Figure 4 a,b) where the mean ER rate at Site 2 (-5.5 ± 0.1 g $O_2/m^2/d$, Figure 4a,b) was greater (more negative, $p < 0.001$) than the average for Site 1(-4.5 ± 0.1 g $O_2/m^2/d$). GPP and ER were highly correlated at both Site 1 ($r^2 = 0.91$, $p < 0.001$) and 2 ($r^2 = 0.83$, $p < 0.001$) despite a lack of correlation between K_{600} and ER, suggesting a low probability of spurious correlation between metabolic measures. Both P:R values and rates of NEP suggested steady-state metabolic character at Site 1; P:R was statistically similar to 1 (0.97, $p > 0.05$, Figure 3c) and a mean NEP not different from zero (-0.022 ± 0.01 g C/m^2, $p > 0.05$, Figure 3e). Site 2 displayed greater autotrophic dominance relative to Site 1, with a P:R value exceeding 1 (1.15, $p < 0.001$, Figure 3d), and a positive rate of NEP (0.3 ± 0.02 g C/m^2, $p < 0.001$, Figure 3f).

Quantile regression indicated that 76% (CI = 70% - 84%) of GPP was used as AR at Site 1, compared to the 64% (CI = 60% - 72%) at Site 2 over the course of sampling (Figure S3). Moreover, AR dominated ER (Figure 4 c,d), representing a strikingly consistent proportion of total respiration at each site (74 and 75% at Sites 1 and 2, respectively, Figure 4e,f). The combination of lower GPP and AR_f at Site 1 resulted in a significantly lower ($p < 0.001$) mean rate of NPP (0.5 ± 0.01 g $C/m^2/d$, Figure 3g) when compared to the downstream site (0.97 ± 0.02 g $C/m^2/d$ Figure 3h). Summation of NEP across the study at each site indicated a net carbon

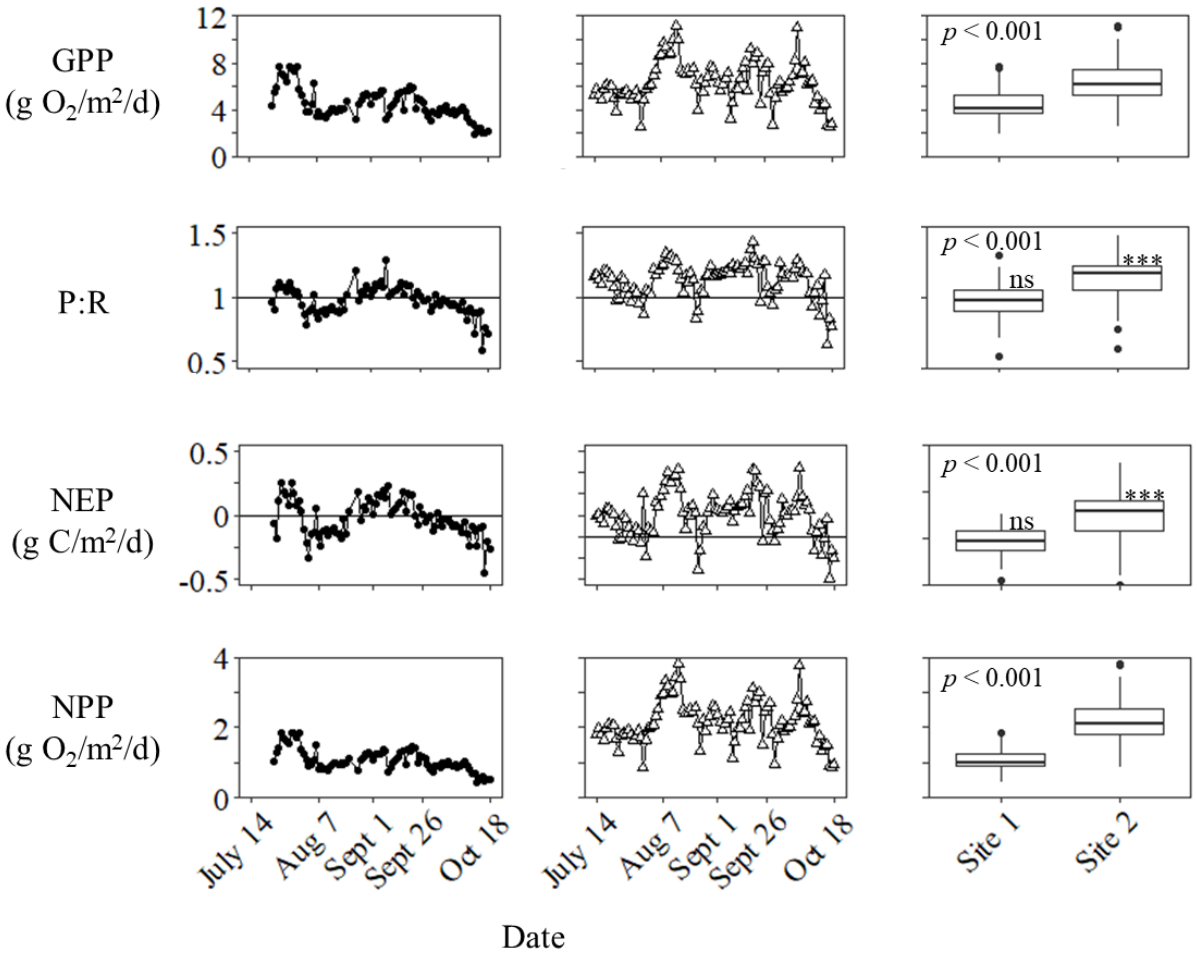

Figure 3: Trends in (a,b) GPP, (c,d) P:R, (e,f) NEP and (g,h) NPP for Sites 1 (closed circles, left hand column) and 2 (open triangles, middle column). Box plots display distribution of data at each site and differences between values are reported using written p-values. Results of t-tests for location (NEP=0; P:R=1) are indicated as not significant (ns), $p > 0.05$; *, $p < 0.05$; **, $p < 0.01$; ***, $p < 0.001$.

input at Site 1 of 1.2 g C/m^2, while at Site 2 NEP accounted for 26 g C/m^2 over the same time frame.

Spatial Differences in nutrient dynamics

Relative differences in the concentrations and delivery of dissolved solutes generally suggested that Site 1 was nutrient-rich compared to Site 2. Loads for NO_3-N at Site 1 (61 ± 4.9 kg/d) were greater than loads delivered to the downstream site (27 ± 34.4 kg/d, $p < 0.001$, Figure 5a,b). Compared to those for NO_3-N, loads for NH_4-N were 5 to 30-fold lower at either site, but delivery of NH_4-N to Site 1 (8.4 ± 1.02 kg/d) was nearly 10x that observed for Site 2 (0.9 kg/d, Figure S4b). In contrast, while the mean SRP load at Site 1 (10.1 ± 39 kg/d) was similar to Site 2 (12 ± 1.7 kg/d, $p > 0.05$), SRP loads at Site 2 exceeded those at Site 1 on 66% of sampling dates (Figure S4c). Calculated nutrient demand for N ($U_{dem\text{-}N}$) varied from 60.3 to 294.3 mg N/m^2/d across the two sites (Figure 5c,d) while that for P ($U_{dem\text{-}P}$) ranged from 8.34 to 40.69 mg P/m^2/d. Following from trends in NPP, calculated rates were lower at Site 1 (99.5 ± 5.1 and 13.7 ± 0.7 for N and P, respectively) compared to Site 2 (195.2 ± 7.7 and 27.0 ± 1.0 for N and P, respectively).

Combined influences of riverine loading and calculated $U_{dem\text{-}N}$ was reflected in substantial differences in $k_{eff\text{-}NO3}$; the rate constant at Site 2 (0.73 ± 0.22 km^{-1}) exceeded the mean $k_{eff\text{-}NO3}$ at Site 1 (0.065 ± 0.008 km^{-1}) by more than an order of magnitude ($p < 0.01$, Figure 5e,f). Similarity, mean $k_{eff\text{-}NH4}$ at Site 2 (10.45 ± 1.42 km^{-1}) was over twenty-fold greater than at Site 1 (0.40 ± 0.03 km^{-1}, $p < 0.001$) and illustrated a putative demand for NH_4-N an order of magnitude greater than is supplied by advective transport.

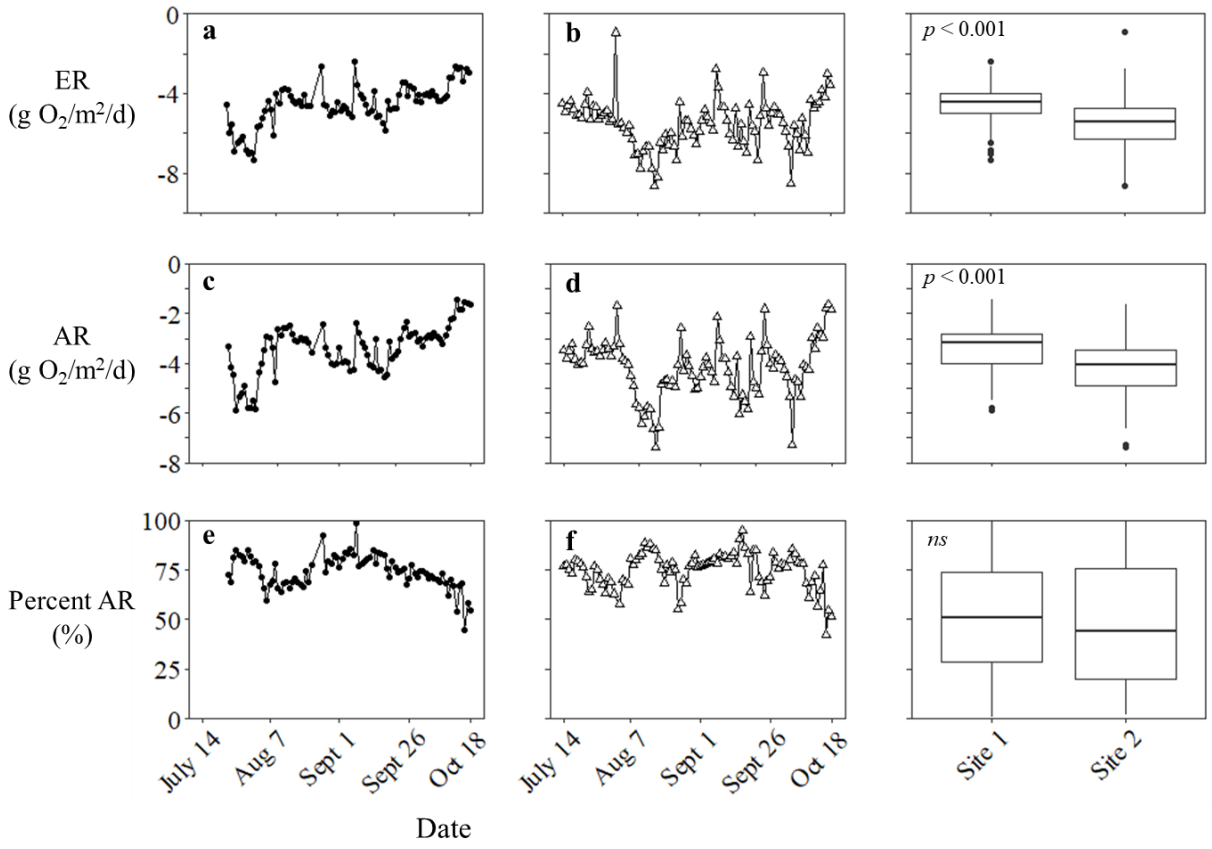

Figure 4: Trends in (a,b) ER, (c,d) AR, (e,f) and percent AR for Sites 1 (closed circles, left hand column) and 2 (open triangles, middle column). Box plots display distribution of data at each site and p-values reflect t-tests for differences between means.

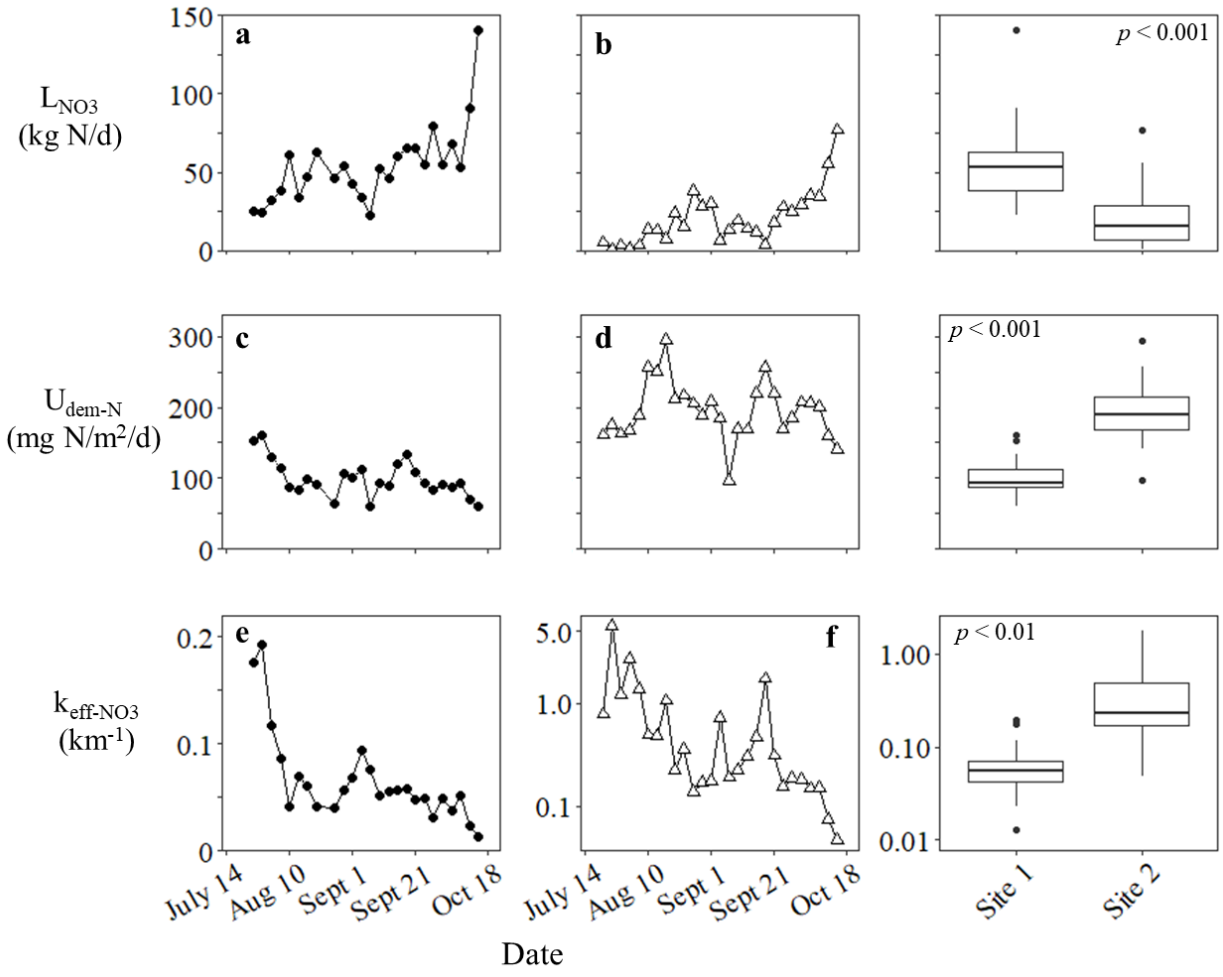

Figure 5: Calculated NO_3-N loads (L_{NO3}, kg/d, a,b), derived measures of N demand (U_{dem-N}, mg/m^2/d, c,d), and respective longitudinal uptake rates ($k_{eff-NO3}$, km^{-1}, e,f) for Sites 1 (closed circles, left hand column) and 2 (open triangles, middle column). Box plots display distribution of data at each site and differences between values are assessed using p-values.

Reach-Scale nutrient dynamics

The reach of river extending between the two sites acted a material sink (i.e., $U_{eff} < 0$) for both NO_3-N (Figure 6A) and NH_4-N (Figure S5a) over the duration of sampling, while displaying temporal variability in the tendency to act as a sink or source for SRP (Figure S6a). The effective solute flux for NO_3-N ($U_{eff\text{-}NO3}$) was -66 ± 5 mg/m^2/d (Figure 6a) with all individual values negative, reflecting sink activity during the entirety of the sampling duration. Upstream and downstream assessment of river flow revealed a directional temporal change in net inflow, with the 20-km of river switching from a gaining reach early in summer to a losing reach for the final two months of sampling (Figure S7). At initiation of sampling, the reach was gaining ~7 m^3/s (37% of flow at Site 1), after which it gained progressively less water into early August and then began losing water with as much as 22% of inflow lost by the end of the sampling season (Figure S7). Associated with increasing magnitude of flow reduction, change in NO_3-N load due to hydrologic exchange ($U_{eff\text{-}hydro\text{-}NO3}$) became increasingly influential, eventually accounting for 87% of load declines at the end of sampling (Figure 6b).

Over the first month of sampling during which ΔQ was positive (July 13 – August 20), $U_{eff\text{-}hydro\text{-}NO3}$ was positive and concomitant net negative $U_{eff\text{-}NO3}$ values served as a conservative measure of biological uptake of NO_3-N ($U_{eff\text{-}bio\text{-}NO3}$). During periods when ΔQ was positive, $U_{eff\text{-}bio\text{-}NO3}$ must account for 100% of changes in N load given that inflow resulted in an unknown but positive contribution to the load reaching Site 2. Despite augmented N loads delivered to Site 2, $U_{eff\text{-}bio\text{-}NO3}$ averaged -58.0 ± 6.87 mg/m^2/d during that period (Figure 6c), a magnitude of areal N removal not different than the mean value measured over the remainder of the study (-57.26 ± 5.43 mg/m^2/d, $p > 0.05$), indicating continued biological contribution to load reduction.

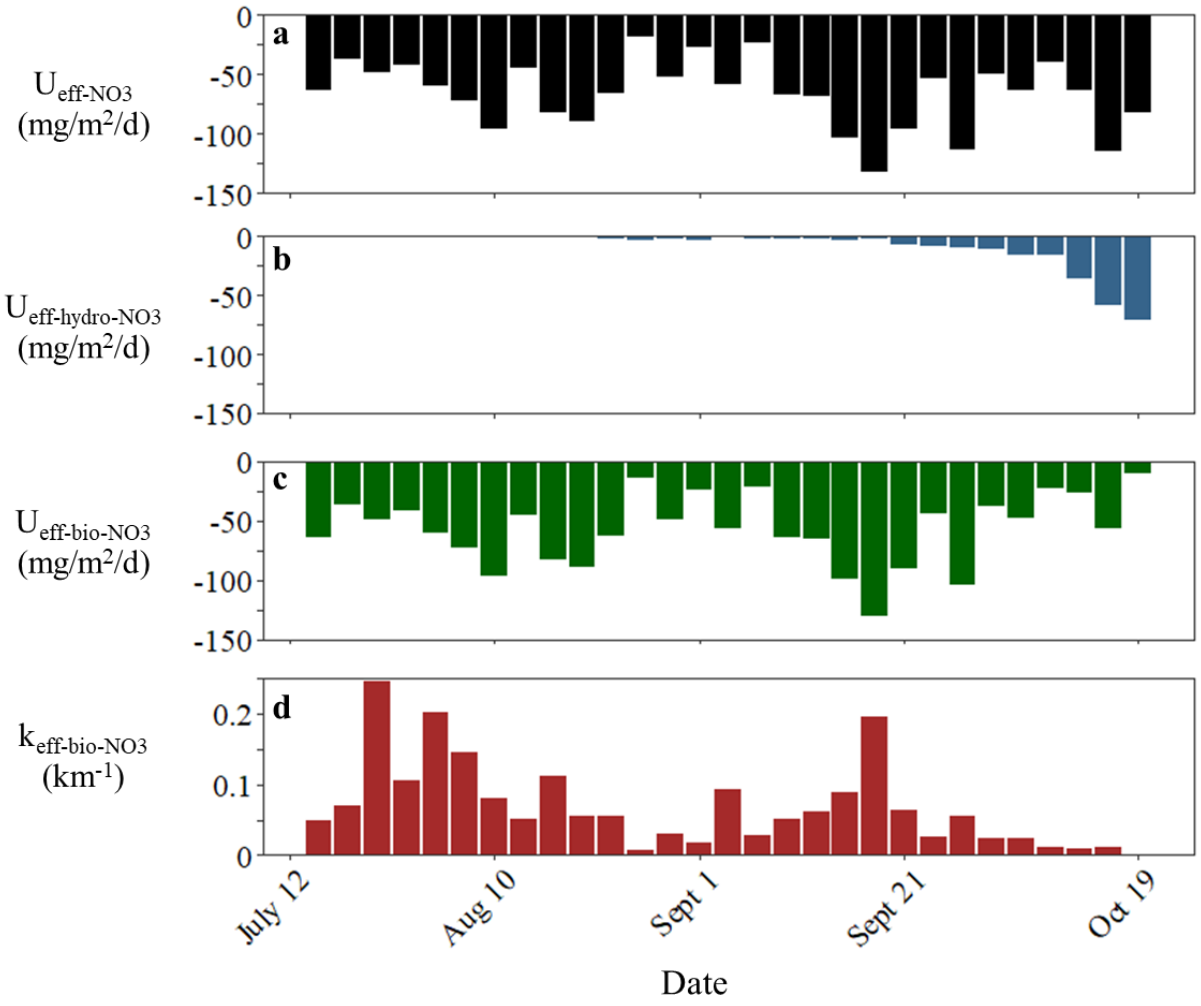

Figure 6: Temporal changes in (a) $U_{eff\text{-}NO3}$, (b) $U_{eff\text{-}hydro\text{-}NO3}$, (c) $U_{eff\text{-}bio\text{-}NO3}$, and (d) $k_{eff\text{-}bio\text{-}NO3}$ derived from mass balance assessments at the reach scale during the growing season. Lack of data for $U_{eff\text{-}hydro\text{-}NO3}$ prior to August 14 reflects net hydrologic gain contributing to increased downstream loads not measured during out study.

Variation in $U_{eff\text{-}bio\text{-}NO3}$ was poorly related to any metabolic measure (i.e., NEP, NPP) specific to either site and instead was best explained by weighted combined metabolic activity from Site 1 (30%) and 2 (70%), including NEP ($r^2 = 0.22$, $p < 0.01$, Figure 7A) and NPP ($r^2 = 0.29$, $p < 0.01$). When NPP was represented as a corresponding $U_{dem\text{-}N}$ values, the significant relationship with $U_{eff\text{-}NO3}$ ($r^2 = 0.29$, $p < 0.01$, Figure 7B) displayed a range of values for $U_{dem\text{-}N}$ similar to that of $U_{eff\text{-}NO3}$ but with an average value (147.7 ± 6.06 mg/m^2/d) approximately three-fold greater than that derived from empirical mass-balance measures (-57.26 ± 5.44 mg/m^2/d). While site-specific measures of $k_{eff\text{-}NO3}$ suggested N consumption exceeded supply early in the growing season at Site 2 (Figure 5f), $k_{reach\text{-}bio\text{-}NO3}$, a proportional measure of reach-scale uptake, suggested an average net consumption of approximately 6% (0.06 ± 0.01 km^{-1},) with rates ranging between 10 and 25% during only 6 of 29 days (Figure 6d).

Discussion

Metabolic and Biogeochemical Differences between Sites

Rates of GPP were high at both sites, greater than 64 of 72 streams addressed by the second Lotic Intersite Nitrogen Experiment (LINX II, Bernot et al. 2010), but were lower than those observed in the iconic autotrophic systems including Sycamore Creek, AZ (8.5 g O_2/m^2/d, Busch and Fisher 1981) and Deep Creek, ID (10-11 g O_2/m^2/d, Minshall et al. 1975, Minshall 1978). Rates for GPP in the UCFR were similar to those reported for both the sewage-enriched Oria River, Spain, prior to the installation of a waste water treatment plant (Arroita et al. 2019), and well-lit reaches of the Portneuf River, Idaho (Marcarelli et al. 2009). Rates of ER, on the other hand, fell within the range of values typical of many other streams (Hall and Tank 2003, Marcarelli et al. 2009, Covino et al. 2018) and were comparable to the median value reported by Bernot et al. (2010).

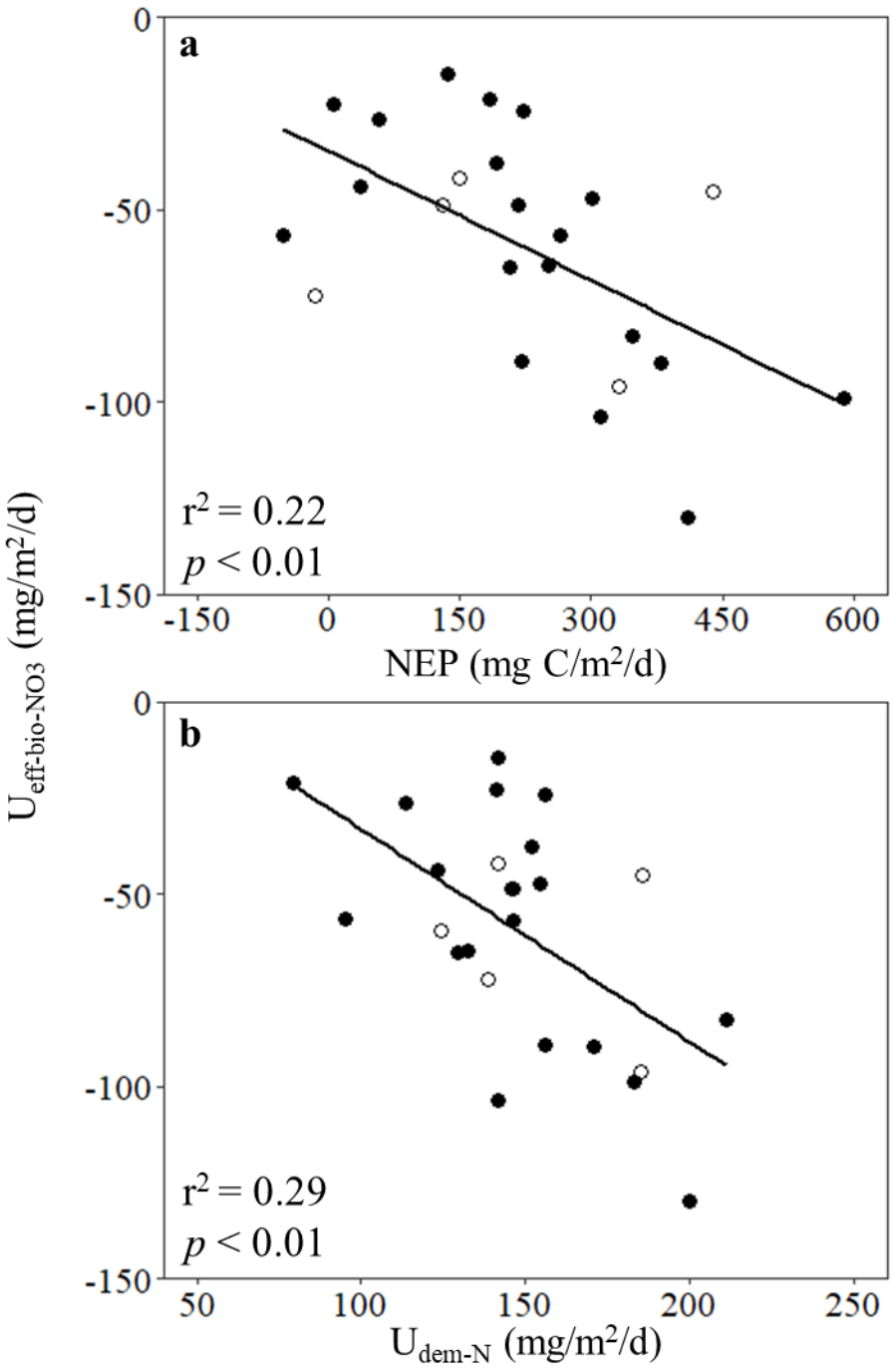

Figure 7: Relationship between $U_{eff\text{-}bio\text{-}NO3}$, (a) weighted NEP, and (b) autorophic N demand ($U_{dem\text{-}N}$) calculated from weighted NPP. Open circles represent data during which ΔQ was positive and closed circles represent data during which ΔQ was negative. Respective equations are (a) $U_{eff\text{-}bio\text{-}NO3} = -40.87 - 0.08NEP$ and (b) $U_{eff\text{-}bio\text{-}NO3} = 22.30 - 0.55U_{dem\text{-}N}$.

Both GPP and ER where substantially greater at Site 2 compared to the Site 1. Derived metabolic parameters (P:R, NEP, NPP) illustrated a shift in the metabolic balance from upstream steady-state to an autotrophic system (i.e., P:R > 1, Odum 1956, Fisher and Likens 1973) further downstream. At Site 1, BOM and Chl a abundances remained relatively constant through the growing season, congruent with the temporally unchanged rates of GPP and ER. A Mean P:R ratio similar to 1 and a mean rate of NEP near zero further suggest metabolic steady state. Metabolic character then shifted longitudinally to greater autotrophy, where P:R values were >1 and rates of NEP were positive. Although metabolic activity associated with Site 2 indicated biomass accumulation, measured BOM and Chl a standing crops did not increase, and instead decreased during the study. Banish (2017) documented a directional decline in both BOM and Chl a through time at nearby sites in the UCFR, similar to the trend exhibited by BOM at Site 2. In my study, BOM declined markedly at Site 2, but the corresponding decline in Chl a was far more muted, resulting in a corresponding increase in Chl a:BOM values that was progressive and significant. Together, these data suggest that BOM at Site 2 became noticeably more autotrophic in character even as its abundance declined.

Declining biomass coupled to autotrophic metabolic state requires that organic matter be exported from the ecosystem. In his study of the UCFR, Banish (2017) measured substantial algal drift early in the growing season, suggesting that downstream export of organic matter accounted for the decline in measured BOM observed during our study as well. The downstream export of BOM is not uncharacteristic of streams rich in filamentous algae, where changes in discharge may directly influence BOM abundance (Power and Stewart 1987, Blinn et al. 1995, Shannon et al. 1996). The export of BOM in algae rich rivers is not, however, directly tied to

senescence, and algal drift can contribute to total OM (Gubelit and Berezina 2010) and food-web dynamics (Power 1990) in downstream reaches.

AR_f estimates fell in the upper range of reported values (Hall and Beaulieu 2013, Arroita et al. 2019) and were most similar to rivers enriched in nutrients (Arroita et al. 2019) and those draining agricultural landscapes (Griffiths et al. 2013). Values are most different from those documenting heterotrophic, allochthonous-based streams, including Walker Branch, TN (Mulholland 1997) and the Portneuf River, ID (Marcarelli et al. 2010). Among sites, AR comprised a consistent and substantial portion of ER, where GPP and ER were also highly correlated, suggesting that autotrophs accounted for a substantial portion of the metabolic signal. This close relationship between GPP and ER is demonstrated in other well-lit rivers, including the Necker River of eastern Switzerland (Uehlinger and Naegeli 1998). An explanation for the relevance of AR in the UCFR is the overall abundance of primary producers, and the substantial AR_f values exhibited at either site. High AR relative to HR suggests active production and processing of autochthonous C with the potential for HR to be supported by autochthonously-derived detritus (Thorp and Delong 2002, Bunn et al. 2003). Others have emphasized the importance of autochthonous C for stream food webs (Finlay et al. 1999) and while little is known about the basis of the food web in the UCFR, Peipoch and Valett (2019) documented a bottom-up enhancement of energy flow as a result of seasonal algal proliferation. In any case, the high rates of GPP relative to rates of ER, when considered in tandem with the proportion of ER attributed to AR, suggest that carbon dynamics (NEP) capture a predominantly autotrophic signal.

Due to the observed metabolic steady-state, nutrient cycling internal to algal biomass may be sufficient for continued maintenance. Mulholland et al. (1994) and Steinman et al. (1995)

demonstrated how internal cycling can be an important source of nutrients in periphyton communities with low chlorphyll:biomass ratios. A similar relationship between pigment content and algal biomass at Site 1 supports the premise that nutrient recycling may be important to the maintenance of autotrophic biomass. At the same time, effective uptake rate constants ($k_{eff\text{-}NO3}$) suggest that NPP at Site 1 could be supported through consumption of less than 10% of the advected NO_3-N load for most dates considered. This condition contrasts with that observed for Site 2 where the river was autotrophic (i.e., P:R > 1), NEP was positive, Chl:BOM ratios increased over time, and putative uptake ($k_{eff\text{-}NO3}$) often equaled or exceeded supply.

Corresponding to observed metabolic differences, each site exhibited distinctly different biogeochemical character, with greater solute concentrations at Site 1, but greater biogeochemical fluxes occurring at Site 2. Monitoring of the UCFR associated with the Long-term Research in Environmental Biology (LTREB) program suggests that Site 1 has historically acted as a source for NO_3-N of unknown origin. High concentrations of NO_3-N could be linked to agriculture (Tri-State Water Council 2009, Clark Fork Coalition 2016) but recent findings suggest that Lost Creek and the surrounding landscape upstream of Site 1 may be a substantial source of DIN originating from waste water treatment ponds (H.M. Valett, unpublished data). Concentrations of NO_3-N measured during the 2020 growing season were typical of these observed historically for these locations (Tri-State Water Council 2009). In contrast to Site 1, Site 2 acted as a sink for NO_3-N delivered from the upstream reach and displayed strikingly different biogeochemical behavior corresponding to shift in metabolic character.

Reach-Scale Mechanisms Contributing to Site-Specific Differences

During the first month of sampling the reach gained water. In mid-August, the segment switched to a losing reach and water loss accounted for nearly 90% of load change between the

two sites late in the season. Regardless of the concentration of NO_3-N associated with hydrologic inputs in the first month of sampling, absolute changes in NO_3-N load over the area of the reach ($U_{eff\text{-}NO3}$) were consistently negative, and continually attributed to biological uptake ($U_{eff\text{-}bio\text{-}NO3}$, Figure 6). Even as a conservative measure of biological uptake, consistently negative values of $U_{eff\text{-}bio\text{-}NO3}$ exemplify the tendency for this reach to act as a biological sink.

My measures of $U_{eff\text{-}NO3}$ fall within the range of values previously reported for this reach (Valett et al. in review), as well as those in Walker Branch, TN (Roberts and Mulholland 2007), Mississippi River pools (James et al. 2014), and an array of 1^{st}-5^{th} order streams (Ensign and Doyle 2006). The positive relationship between $U_{eff\text{-}bio\text{-}NO3}$ (a measure derived from changes in NO_3-N load), and NEP or NPP (measures derived from DO dynamics) suggest that biological assimilation is an important control on chemical availability. Moreover, metabolic estimates suggest that a substantial portion of ER is attributed to AR (~75%), making NEP a measure reflecting predominantly autotrophic energetics. Therefore, the correlations between $U_{eff\text{-}bio\text{-}NO3}$ and NEP or NPP suggest that organic matter production by autotrophs reduces material N load through space, thus accounting for measured differences between sites. Additionally, the general agreement between values for $U_{dem\text{-}N}$ (derived from metabolic estimates) and $U_{eff\text{-}bio\text{-}NO3}$ suggests that autotrophic N processing is a dominant mechanism accounting for changes in $U_{eff\text{-}NO3}$.

Although others have documented the relationship between reductions in material load and metabolism (Hall and Tank 2003, Roberts and Mulholland 2007), it is often the case that the cumulative impact of heterotrophic and autotrophic demand account for these changes (Hoellein et al. 2007, Johnson and Tank 2009). However, weighted estimates of $U_{dem\text{-}N}$ suggest that autotrophs require nearly three-fold what was measured as $U_{eff\text{-}NO3}$, suggesting unmeasured sources of DIN likely contribute to autotrophic assimilation. Likewise, mass-balance calculations

reflect net changes in N loads that may be influenced by an array of pools and transformations that alter availability over the reach.

A shortcoming of mass-balance methods such as those employed here are that they do not individually account for assimilatory and dissimilatory pathways that influence material fate. Additionally, my approach cannot account for solute contributions associated with inputs of surface or groundwater that occur at the reach scale. Thus, when integrated over the area of the reach (e.g., as U_{eff}), biological influence on supply is underestimated, especially when compared to gross measures derived from tracer approaches (Peterson et al. 2001, Webster et al. 2003, Tank et al. 2018).

As a potential source for DIN, N-fixation occurs in downstream reaches of the UCFR (Feijo de Lima et al. unpubl.), but rates of N-fixation in streams are not frequently measured (Marcarelli et al. 2008) and are poorly constrained. Under conditions of DIN scarcity, N-fixation contributed to N availability in open-channel, well-lit streams (Grimm and Petrone 1997), as well as other rivers draining the Rocky Mountains (Marcarelli and Wurtsbaugh 2006). In addition, N-fixing taxa have been shown to increase with P enrichment (Marcarelli and Wurtsbaugh 2006, 2007), and given the high availability of P at each site, N-fixation is likely contributing to N uptake and availability, especially during the summer months when water is warm and water column inorganic N greatly depleted.

Dissimilatory processes such as nitrification may contribute to NO_3-N loading, while denitrification may be reducing NO_3-N availability. Given the concentrations of NH_4-N at the upstream site, and the high autotrophic biomass over the reach, it is probable that nitrification is contributing to NO_3-N availability. Dodds and Kemp (2001) noted high nitrification rates associated with filamentous algae in an agriculturally influenced prairie stream, and Dodds et al.

(2000) found N cycling by autotrophs in the same system to be a dominant mechanism influencing N turnover rates. Nitrification removed NH_4-N in a number of tropical streams in northeastern Puerto Rico (Koenig et al. 2017), but in contrast, other small Rocky Mountains streams with DIN compositions similar to ours have low nitrification fluxes relative to NH_4-N uptake (Day and Hall 2017). Ultimately, many factors control nitrification aside from DIN availability alone, including DO concentrations (Kemp and Dodds 2002), and the availability of C (Arango and Tank 2008). More data is required to assess the influence of nitrification in the UCFR.

Dissimilatory conversion of NO_3-N to gaseous forms by denitrification may influence mass balance along the study reach. Other streams draining agricultural landscapes such as the Sangamon, Ambarras, and Kaskaskia rivers of Illinois (Royer et al. 2004, Schaller et al. 2004), or the Kalamazoo River in southwestern Michigan (Inwood et al. 2005) have high rates of denitrification associated with elevated concentrations of NO_3-N. However, NO_3-N concentrations in those studies are greater (50-100 fold) than presented here, and given the oxic conditions associated with this reach of the UCFR, denitrification may not be a highly relevant fate for NO_3-N. However, no data regarding the role of denitrification in this river are currently available.

A portion of $U_{dem\text{-}N}$ may be supplied as NH_4-N, although values for $U_{eff\text{-}NH4}$ suggests that daily average uptake up NH_4-N is small when compared to that of NO_3-N (Figure S6). Nutritional subsidies associated with surface and groundwater inputs may contribute to the DIN pool, but hydrologic conditions suggest that this premise applies only during the first month of sampling. Instead, internal processing and recycling of N must influence net N cycling and the relationships between N supply and demand over the reach, especially given the differences in

OM abundance and nutrient concentrations observed between sites. Reach-scale measures of longitudinal uptake rates ($k_{reach\text{-}bio\text{-}NO3}$) suggest that 6 to 20% of the available NO_3-N load is biologically consumed every kilometer, while estimates of $U_{dem\text{-}N}$ indicate that biological demand is nearly triple that of NO_3-N supply. These two measures, when considered in tandem, suggest that internal processes (namely N-fixation, nitrification, and mineralization) must be contributing to the DIN pool, although the relative importance of each process is unknown.

Although internal recycling of nutrients may be efficient enough to account for the differences between metabolic demand and material supply at Site 1 where metabolic steady-state led to unchanging BOM, the autotrophic character of Site 2 must be supported not only by N generated from recycling along the reach, but by the potential combination of N in transport and autochthonous N production (i.e., fixation). While HR represented ca. 25% of ER, inefficiencies of heterotrophic organic matter processing suggests that mineralization may be a quantitatively important flux. Following the same stoichiometric approach to calculating $U_{dem\text{-}N}$ from NPP, I estimated potential mineralization rates using heterotrophic growth efficiency (Del Giorgio et al. 1997) and weighted HR values. These estimates suggest that heterotrophic mineralization of autochthonous detrital matter would support biological demand over the study reach. On average, mineralization could contribute an additional 160.7 ± 39.8 mg N/m^2/d to the UCFR while the difference between $U_{dem\text{-}N}$ and $U_{eff\text{-}bio\text{-}NO3}$ averaged 88.3 ± 5.5 mg N/m^2/d. Actual growth efficiencies and C:N of mineralized detritus in this river are unknown. Documented mineralization rates for stream ecosystems are sparse (Webster et al. 2009, Cheever et al. 2012) and ultimately tracking interconnected sources and fates of inorganic N in this river would require 15N tracers.

Conclusion

My study illustrated distinct differences in the metabolic and nutritional character between two sites separated by 20 km of river. Site 1 was characterized by low, unchanging biomass, steady-state metabolic character, and high nutrient availability, while Site 2 had high biomass, an autotrophic metabolic character, and lower nutrient availability. At the reach-scale, autotrophic assimilation was a dominate mechanism accounting for decreasing N loads between sites. Along the reach, metabolic demand for N was not met by NO_3-N loads alone. Instead, other internal processes (i.e., N-fixation, nitrification, and mineralization) must have been contributing to N availability. I suggest that future research aiming to address N dynamics in the UCFR employ a 15N tracer approach to individually assess the influence of each assimilatory and dissimilatory pathway.

References

Appling, A. P., R. O. Hall, C. B. Yackulic, and M. Arroita. 2018. Overcoming Equifinality: Leveraging Long Time Series for Stream Metabolism Estimation. J. Geophys. Res.: Biogeosci. 123:624–645.

Arango, C. P., and J. L. Tank. 2008. Land use influences the spatiotemporal controls on nitrification and denitrification in headwater streams. J. N. Amer. Benthol. Soc. 27:90–107.

Arroita, M., A. Elosegi, and R. O. Hall. 2019. Twenty years of daily metabolism show riverine recovery following sewage abatement. Limnol. Oceanogr. 64:S77–S92.

Bernot, M. J., D. J. Sobota, R. O. Hall, P. J. Mulholland, W. K. Dodds, J. R. Webster, J. L. Tank, L. R. Ashkenas, and others. 2010. Inter-regional comparison of land-use effects on stream metabolism. Freshw. Biol. 55:1874–1890.

Blinn, D. W., J. P. Shannon, L. E. Stevens, and J. P. Carder. 1995. Consequences of Fluctuating Discharge for Lotic Communities. J. N. Amer. Benthol. Soc. 14:233–248.

Bott, T. L., J. Brock, C. . Cushing, S. V. Gregory, D. King, and R. C. Peterson. 1979. A comparison of methods for measuring primary productivity and community respiration in streams. Hydrobiologia 62:65–69.

Bunn, S. E., P. M. Davies, and M. Winning. 2003. Sources of organic carbon supporting the food web of an arid zone floodplain river. Freshw. Biol. 48:619–635.

Busch, D. E., and S. G. Fisher. 1981. Metabolism of a desert stream. Freshw. Biol. 11:301–207.

Cade, B. S., and B. R. Noon. 2003. A gentle introduction to quantile regression for ecologists. Front. Ecol. Environ. 1:412–420.

Cheever, B. M., E. B. Kratzer, and J. R. Webster. 2012. Immobilization and mineralization of N and P by heterotrophic microbes during leaf decomposition. Freshw. Sci. 31:133–147.

Clark Fork Coalition. 2016. Upper Clark Fork Aquatic Restoration Strategy II.

Tri-State Water Quality Council. 2009. Final report: The Clark Fork river voluntary nutrient reduction program 1998-2008:1–59.

Covino, T. P., E. S. Bernhardt, and J. B. Heffernan. 2018. Measuring and interpreting relationships between nutrient supply, demand, and limitation. Freshw. Sci. 37:448–455.

Day, N. K., and R. O. Hall. 2017. Ammonium uptake kinetics and nitrification in mountain streams. Freshw. Sci. 36:41–54.

Dere Şükran, Tohot GÜNEŞ, R. Sivac. 1998. Spectrophotometric Determination of Chlorophyll - A, B and Total Carotenoid Contents of Some Algae Species Using Different Solvents. Turk. J. Botany 22:13–18.

Dodds, W. K., M. A. Evans-White, N. M. Gerlanc, L. Gray, D. A. Gudder, M. J. Kemp, A. L. López, D. Stagliano, and others. 2000. Quantification of the nitrogen cycle in a prairie stream. Ecosystems 3:574–589.

Dodds, W. K., and M. J. Kemp. 2001. Spatial and temporal patterns of nitrogen concentrations in pristine and agriculturally-influenced prairie streams. Biogeochemistry 53:125–141.

Dodds, W. K., and V. H. Smith. 2016. Nitrogen, phosphorus, and eutrophication in streams. Inland Waters 6:155–164.

Dodds, W. K., V. H. Smith, and B. Zander. 1997. Developing nutrient targets to control benthic chlorophyll levels in streams: A case study of the Clark Fork River. Water Res. 31:1738–1750.

Ensign, S. H., and M. W. Doyle. 2006. Nutrient spiraling in streams and river networks. J. Geophys. Res.: Biogeosci. 111:1–13.

Finlay, J. C., M. E. Power, and G. Cabana. 1999. Effects of water velocity on algal carbon isotope ratios: Implications for river food web studies. Limnol. Oceanogr. 44:1198–1203.

Del Giorgio, P. A., J. J. Cole, and A. Cimbleris. 1997. Respiration rates in bacteria exceed phytoplankton production in unproductive aquatic systems. Nature:148–151.

Griffiths, N. A., J. L. Tank, T. V. Royer, S. S. Roley, E. J. Rosi-Marshall, M. R. Whiles, J. J. Beaulieu, and L. T. Johnson. 2013. Agricultural land use alters the seasonality and magnitude of stream metabolism. Limnol. Oceanogr. 58:1513–1529.

Grimm, N. B., and K. C. Petrone. 1997. Nitrogen fixation in a desert stream ecosystem. Biogeochemistry 37:33–61.

Gubelit, Y. I., and N. A. Berezina. 2010. The causes and consequences of algal blooms: The Cladophora glomerata bloom and the Neva estuary (eastern Baltic Sea). Mar. Pollut. Bull. 61:183–188.

Hall, R. J. O. 2016. Metabolism of Streams and Rivers: Estimation, Controls, and Application. Pages 151–180 *in* J. B. Jones and E. H. Stanley, editors. Stream Ecosystems in a Changing Environment. Academic Press, London.

Hall, R. O., M. A. Baker, E. J. Rosi-Marshall, J. L. Tank, and J. D. Newbold. 2013. Solute-specific scaling of inorganic nitrogen and phosphorus uptake in streams. Biogeosciences 10:7323–7331.

Hall, R. O., and J. J. Beaulieu. 2013. Estimating autotrophic respiration in streams using daily metabolism data. Freshw. Sci. 32:507–516.

Hall, R. O., and E. R. Hotchkiss. 2017. Stream Metabolism. Methods in Stream Ecology: Third Edition 2:219–233.

Hall, R. O., and J. L. Tank. 2003a. Ecosystem metabolism controls nitrogen uptake in streams in Grand Teton National Park, Wyoming. Limnol. Oceanogr. 48:1120–1128.

Hall, R. O., and J. L. Tank. 2003b. Ecosystem metabolism controls nitrogen uptake in streams in Grand Teton National Park, Wyoming. Limnology and Oceanography 48:1120–1128.

Heffernan, J. B., and M. J. Cohen. 2010. Direct and indirect coupling of primary production and diel nitrate dynamics in a subtropical spring-fed river. Limnol. Oceanogr. 55:677–688.

Hoellein, T. J., J. L. Tank, E. J. Rosi-Marshall, S. A. Entrekin, and G. A. Lamberti. 2007. Controls on spatial and temporal variation of nutrient uptake in three Michigan headwater streams. Limnol. Oceanogr. 52:1964–1977.

Huryn, A. D., J. P. Benstead, and S. M. Parker. 2014. Seasonal changes in light availability modify the temperature dependence of ecosystem metabolism in an arctic stream. Ecology 95:2840–2850.

Inwood, S. E., J. L. Tank, and M. J. Bernot. 2005. Patterns of denitrification associated with land use in 9 midwestern headwater streams. J. N. Amer. Benthol. Soc. 24:227–245.

James, W. F., W. B. Richardson, and D. M. Soballe. 2014. Effects of residence time on summer nitrate uptake in mississippi river flow-regulated backwaters. River. Res. Appl. 30:132–133.

Johnson, L. T., and J. L. Tank. 2009. Diurnal variations in dissolved organic matter and ammonium uptake in six open-canopy streams. J. N. Amer. Benthol. Soc. 28:694–708.

Jones, C. S., S. won Kim, T. F. Wilton, K. E. Schilling, and C. A. Davis. 2018. Nitrate uptake in an agricultural stream estimated from high-frequency, in-situ sensors. Environ. Monit. Assess. 190.

Jones, J. B., S. G. Fisher, and N. B. Grimm. 1995. Vertical Hydrologic Exchange and Ecosystem Metabolism in a Sonoran Desert Stream. Ecology 76:942–952.

Kemp, M. J., and W. K. Dodds. 2002. Comparisons of nitrification and denitrification in prairie and agriculturally influenced streams. Ecol. Appl. 12:998–1009.

Koenig, L. E., C. Song, W. M. Wollheim, J. Rüegg, and W. H. McDowell. 2017. Nitrification increases nitrogen export from a tropical river network. Freshw. Sci. 36:698–712.

Koenker, R., and K. F. Hallock. 2001. Quantile regression. Nat. Methods 15:143–156.

Lejeune, K., H. Galbraith, J. Lipton, and L. A. Kapustka. 1996. Effects of metals and arsenic on riparian communities in southwest Montana. Ecotoxicology 5:297–312.

Lynch, J. K., C. M. Beatty, M. P. Seidel, L. J. Jungst, and M. D. Degrandpre. 2010. Controls of riverine CO2 over an annual cycle determined using direct, high temporal resolution pCO2 measurements. J. Geophys. Res.: Biogeosci. 115:1–10.

Marcarelli, A. M., M. A. Baker, and W. A. Wurtsbaugh. 2008. Is in-stream N2 fixation an important N source for benthic communities and stream ecosystems? J. N. Amer. Benthol. Soc. 27:186–211.

Marcarelli, A. M., H. A. Bechtold, A. T. Rugenski, and R. S. Inouye. 2009. Nutrient limitation of biofilm biomass and metabolism in the Upper Snake River basin, southeast Idaho, USA. Hydrobiologia 620:63–76.

Marcarelli, A. M., R. W. Van Kirk, and C. V. Baxter. 2010. Predicting effects of hydrologic alteration and climate change on ecosystem metabolism in a western U.S. river 20:2081–2088.

Marcarelli, A. M., and W. A. Wurtsbaugh. 2006. Temperature and nutrient supply interact to control nitrogen fixation in oligotrophic streams: An experimental examination. Limnol. Oceanogr. 51:2278–2289.

Marcarelli, A. M., and W. A. Wurtsbaugh. 2007. Effects of upstream lakes and nutrient limitation on periphytic biomass and nitrogen fixation in oligotrophic, subalpine streams. Freshw. Biol. 52:2211–2225.

Minshall, C., J. Brock, D. McCullough, R. Dunn, M. McSorley, and R. Pace. 1975. Process Studies Related to the Deep Creek Ecosystem. Reports of 1974 Progress Volume 1:

Minshall, G. W. 1978. Autotrophy in Stream Ecosystems. BioScience 28:767–771.

Mulholland, P. J. 1997. Organic Matter Dynamics in the West Fork of Walker Branch , Tennessee , USA. J. N. Amer. Benthol. Soc. 16:61–67.

Mulholland, P. J., C. S. Fellows, S. K. Hamilton, E. Marti, E. S. Division, O. Ridge, O. Ridge, N. Dame, K. B. Station, H. Corners, N. Zealand, J. Hall, and W. Hole. 2001. Inter-Biome comparison of factors controlling stream metabolism. Freshw. Biol. 46:1503–1517.

Mulholland, P. J., R. O. Hall, D. J. Sobota, W. K. Dodds, S. E. G. Findlay, N. B. Grimm, S. K. Hamilton, W. H. McDowell, and others. 2009. Nitrate removal in stream ecosystems measured by 15N addition experiments: Denitrification. Limnol. Oceanogr. 54:666–680.

Mulholland, P. J., E. R. Marzolf, S. Hendricks, R. V. Wilderson, and A. K. Baybayan. 1995. Longitudinal Patterns of Nutrient Cycling and Periphyton Characteristics in Streams : A Test of Upstream-Downstream Linkage. J. N. Amer. Benthol. Soc. 14:357–370.

Mulholland, P. J., A. D. Steinman, E. R. Marzolf, D. R. Hart, D. L. DeAngelis, and E. R. Marzolf D R Hart. 1994. Effect of Periphyton Biomass on Hydraulic Characteristics and Nutrient Cycling in Effect of periphyton biomass on hydraulic characteristics and nutrient cycling in streams. Oecologia 98:40–47.

Neuman, D., P. Hansen, D. Smith, K. Knutson, and S. Brown. 2008. Development and application of pre-remedial design tool for the clark fork river superfund site. ASMR 2:733–749.

Newbold, J. D., J. W. Elwood, R. V. O'Neill, and W. Van Winkle. 1981. Measuring Nutrient Spiralling in Streams. Canadian Journal of Fisheries and Aquatic Sciences 38:860–863.

O`Dell, J. W. 1993a. Method 353.2, Revision 2.0: Determination of Nitrate-Nitrite Nitrogen by Automated Colorimetry:0–14.

O`Dell, J. W. 1993b. Determination of Ammonia Nitrogen by Semi-Automated Colorimetry:1–14.

O`Dell, J. W. 1993c. Method 365.1, Revision 2.0: Determination of Phosphorus By Semi-Automated Colorimetry. Environmental Monitoring Systems Laboratory:1–15.

Odum, H. T. 1956. Primary Production in Flowing Waters. Limnol. Oceanogr. 1:102–117.

Peipoch, M., and H. M. Valett. 2019. Trophic interactions among algal blooms, macroinvertebrates, and brown trout: Implications for trout recovery in a restored river. River. Res. Appl. 35:1563–1574.

Peterson, B. J., W. M. Wollheim, P. J. Mulholland, J. R. Webster, J. L. Meyer, J. L. Tank, E. Marti, W. B. Bowden, and others. 2001. Control of nitrogen export from watersheds by headwater streams. Science 292:86–90.

Power, M. E. 1990. Effects of fish in river food webs. Science 250:811–814.

Power, M. E., and A. J. Stewart. 1987. Disturbance and Recovery of an Algal Assemblage Following Flooding in an Oklahoma Stream. Am. Midl. Nat. 117:333–345.

Redfield, A. C. 1934. On the Proportions of Organic Derivatives in Sea Water and Their Relation to the Composition of Plankton. University Press of Liverpool, James Johnstone Memorial Volume:1767–192.

Ritchie, R. J. 2008. Universal chlorophyll equations for estimating chlorophylls a, b, c, and d and total chlorophylls in natural assemblages of photosynthetic organisms using acetone, methanol, or ethanol solvents. Photosynthetica 46:115–126.

Roberts, B. J., and P. J. Mulholland. 2007. In-stream biotic control on nutrient biogeochemistry in a forested stream, West Fork of Walker Branch. J. Geophys. Res.: Biogeosci. 112:1–11.

Royer, T. V., J. L. Tank, and M. B. David. 2004. Transport and fate of nitrate in headwater agricultural streams in Illinois. Journal of Environmental Quality 33:1296–1304.

Schaller, J. L., T. V. Royer, M. B. David, and J. L. Tank. 2004. Denitrification associated with plants and sediments in an agricultural stream. J. N. Amer. Benthol. Soc. 23:667–676.

Shannon, J. P., D. W. Blinn, P. L. Benenati, and K. P. Wilson. 1996. Organic drift in a regulated desert river. Can. J. Fish. Aquat. Sci. 53:1360–1369.

Simpson, G. L. 2018. Modelling palaeoecological time series using generalised additive models. Front. Ecol. Environ. 6:1–21.

Smith, V. H., G. D. Tilman, and J. C. Nekola. 1999. Eutrophication: Imapcts of excess nutrient imputs on freshwater, marine, and terrestiral ecosystems. Environ. Pollut. 100:176–196.

Stagliano, D. 2020. Clark Fork River Biomonitoring: Macroinvertebrate community assessments for 2019. U.S. Environmental Protection Agency.

Steinman, A. D., P. J. Mulholland, and J. J. Beauchamp. 1995. Effects of Biomass , Light , and Grazing on Phosphorus Cycling in Stream Periphyton Communities. J. N. Amer. Benthol. Soc. 14:371–381.

Suplee, M. W., V. Watson, W. K. Dodds, and C. Shirley. 2012. Response of Algal Biomass to Large-Scale Nutrient Controls in the Clark Fork River, Montana, United States. JAWRA 48:1008–1021.

Tank, J. L., E. Martí, T. Riis, D. von Schiller, A. J. Reisinger, W. K. Dodds, M. R. Whiles, L. R. Ashkenas, and others. 2018. Partitioning assimilatory nitrogen uptake in streams: an analysis of stable isotope tracer additions across continents. Ecol. Monogr. 88:120–138.

Tank, J. L., E. J. Rosi-Marshall, M. A. Baker, and R. O. Hall. 2008. Are rivers just big streams? A pulse method to quantify nitrogen demand in a large river. Ecology 89:2935–2945.

Thorp, J. H., and M. D. Delong. 2002. Dominance of autochthonous autotrophic carbon in food webs of heterotrophic rivers. Oikos 96:543–550.

Uehlinger, U. R. S., and M. W. Naegeli. 1998. Ecosystem Metabolism , Disturbance , and Stability in a Prealpine Gravel Bed River. J. N. Amer. Benthol. Soc. 17:165–178.

Valett, H. M., S. A. Thomas, P. J. Mulholland, J. R. Webster, C. N. Dahm, C. S. Fellows, C. L. Crenshaw, and C. G. Peterson. 2008. Endogenous and exogenous control of ecosystem function: N cycling in headwater streams. Ecology 89:3515–3527.

Webster, J. R., P. J. Mulholland, J. L. Tank, H. M. Valett, W. K. Dodds, B. J. Peterson, W. B. Bowden, C. N. Dahm, and others. 2003. Factors affecting ammonium uptake in streams - An inter-biome perspective. Freshw. Biol. 48:1329–1352.

Webster, J. R., J. D. Newbold, S. A. Thomas, H. M. Valett, and P. J. Mulholland. 2009. Nutrient uptake and mineralization during leaf decay in streams-a model simulation. Int. Rev. Hydrobiol. 94:372–390.

Wetzel, R. G., and G. E. Likens. 2000. Limnological Analyses. Springer-Verlag, New York.

Supplementary Materials

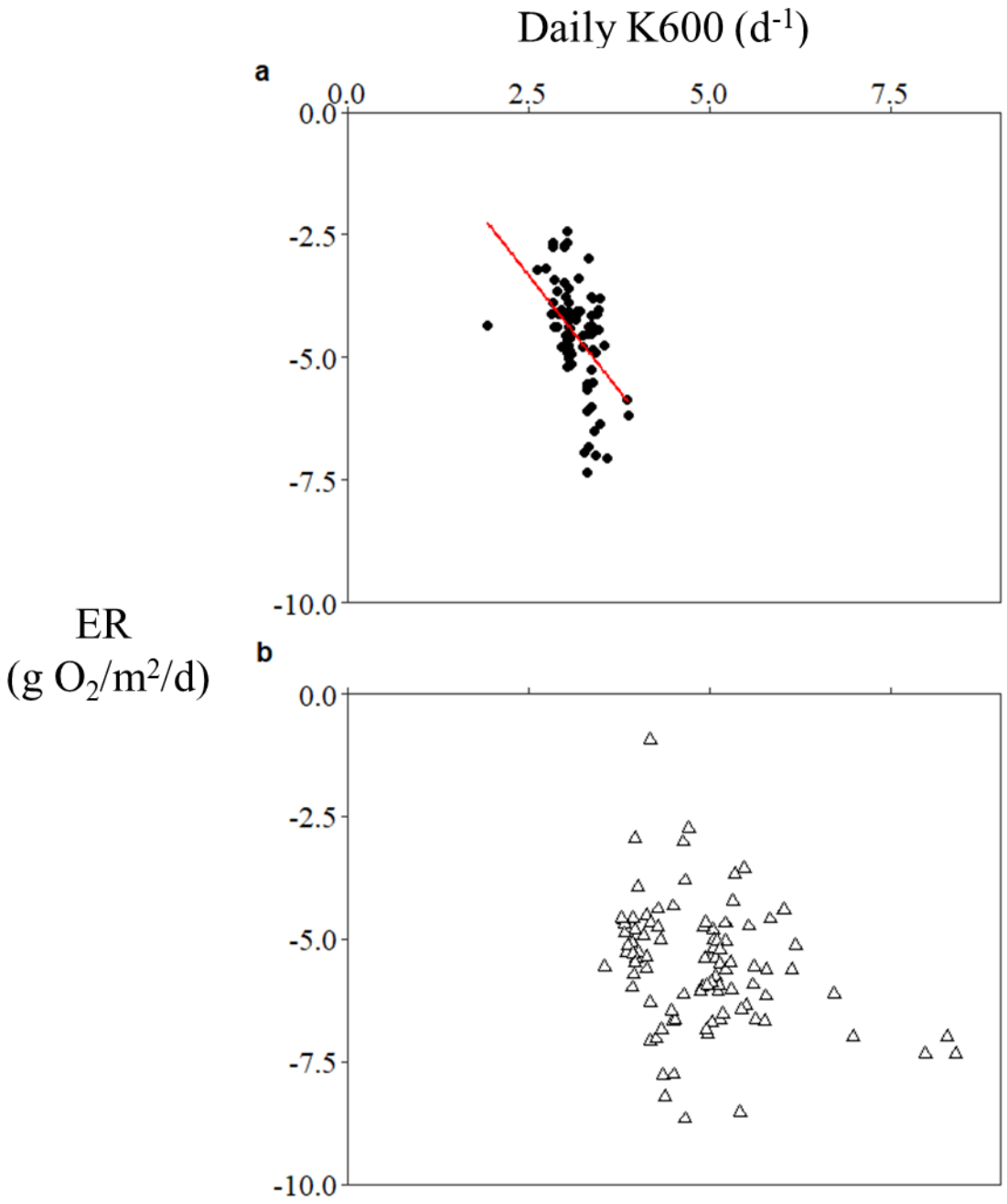

Figure S1: Relationship between daily K600 (d^{-1}) and daily ER (g $O_2/m^2/d$) for Site 1 (black circles, a) and Site 2 (open triangles, b). A weak relationship between the two was found at Site 1 ($r^2 = 0.21$, $p < 0.001$), while no signification relationship was found at Site 2 ($r^2 = 0.06$, $p < 0.01$).

Table S1: A comprehensive list of calculated terms including a brief definition and units.

TERM	DEFINITION	UNITS
L	Instantaneous load	kg/d
ΔL	Net change in load	kg/d
ΔL_{hydro}	Change in load attributed to hydrologic loss	kg/d
ΔL_{bio}	Change in load attributed to biogeochemical processes	kg/d
U_{eff}	Net change in load expressed as effective areal solute flux	$mg/m^2/d$
$U_{eff\text{-}hydro}$	Areal solute flux attributed to hydrologic loss	$mg/m^2/d$
$U_{eff\text{-}bio}$	Areal solute flux attributed to biogeochemical processes	$mg/m^2/d$
k_{eff}	Site-specific measures of effective first-order longitudinal uptake rates	km^{-1}
$k_{reach\text{-}bio}$	effective longitudinal uptake rate attributed to biology	km^{-1}

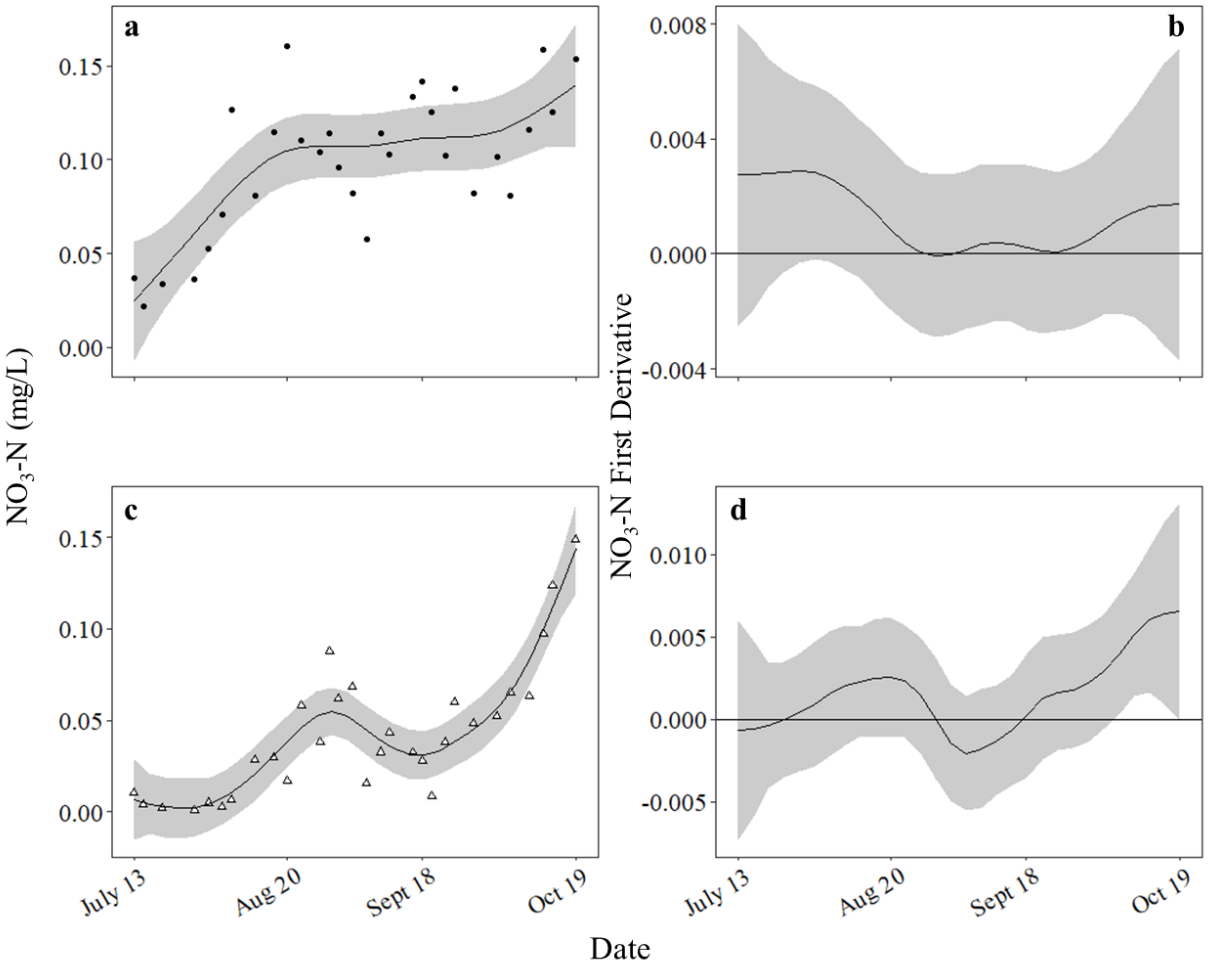

Figure S2: NO_3 concentrations (black dots) at the (a) upstream (c) downstream Sites including best fit GAM (black line) and 95% confidence interval (gray band). First derivatives of best fit GAMs (black line) for the (b) upstream and (d) downstream Sites with 95% simultaneous confidence intervals (gray band). Points of change in the modeled time series are indicated by simultaneous confidence intervals (b) that do not include 0.

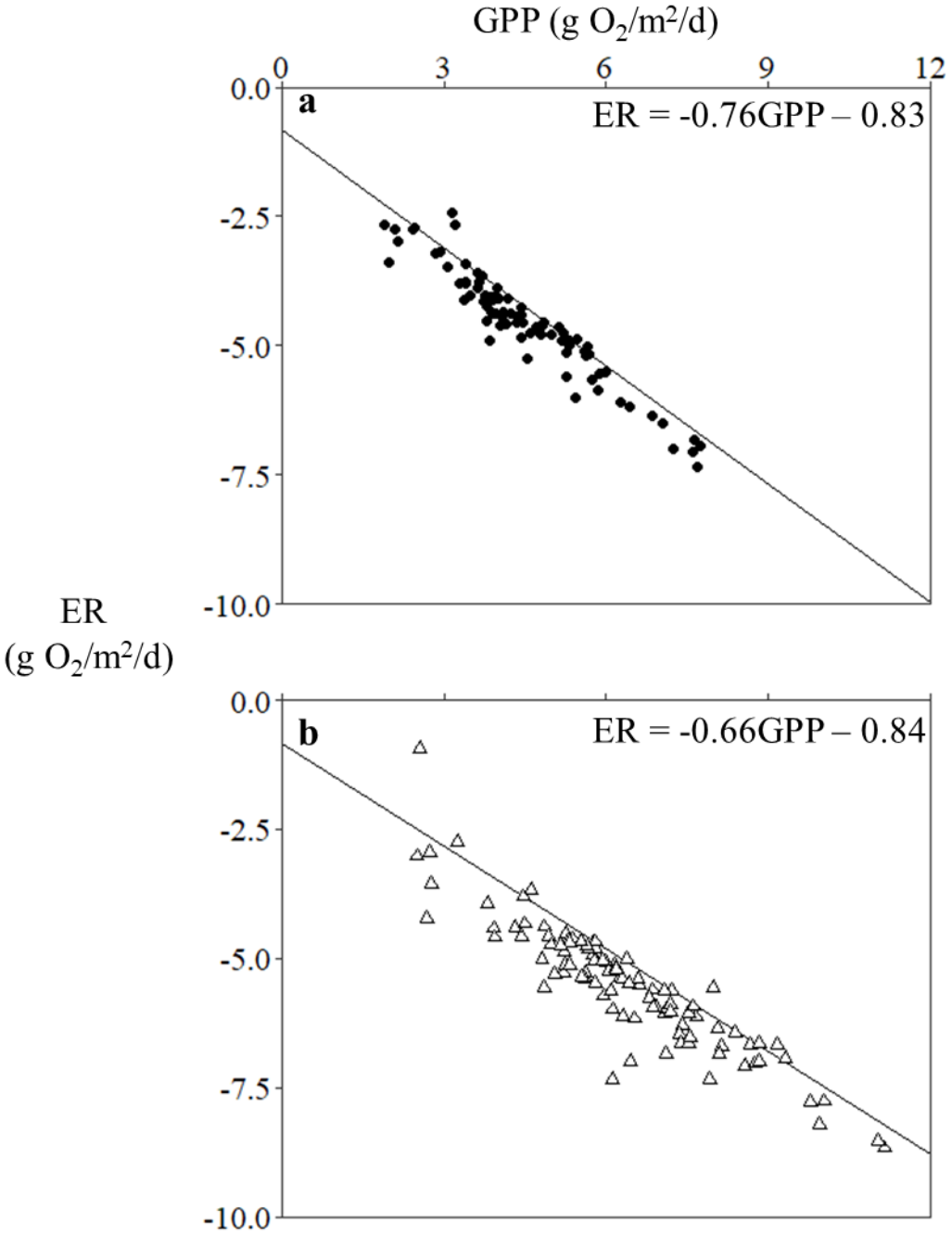

Figure S3: AR_f relationship between GPP and ER for Site 1 (a, closed circles) and 2 (b, open triangles). Points are daily means of GPP and ER and lines represent the 0.9 quantile. Proportion of GPP used as AR indicated by slope of 0.9 quantiles (76 and 66% for Sites 1 and 2, respectively).

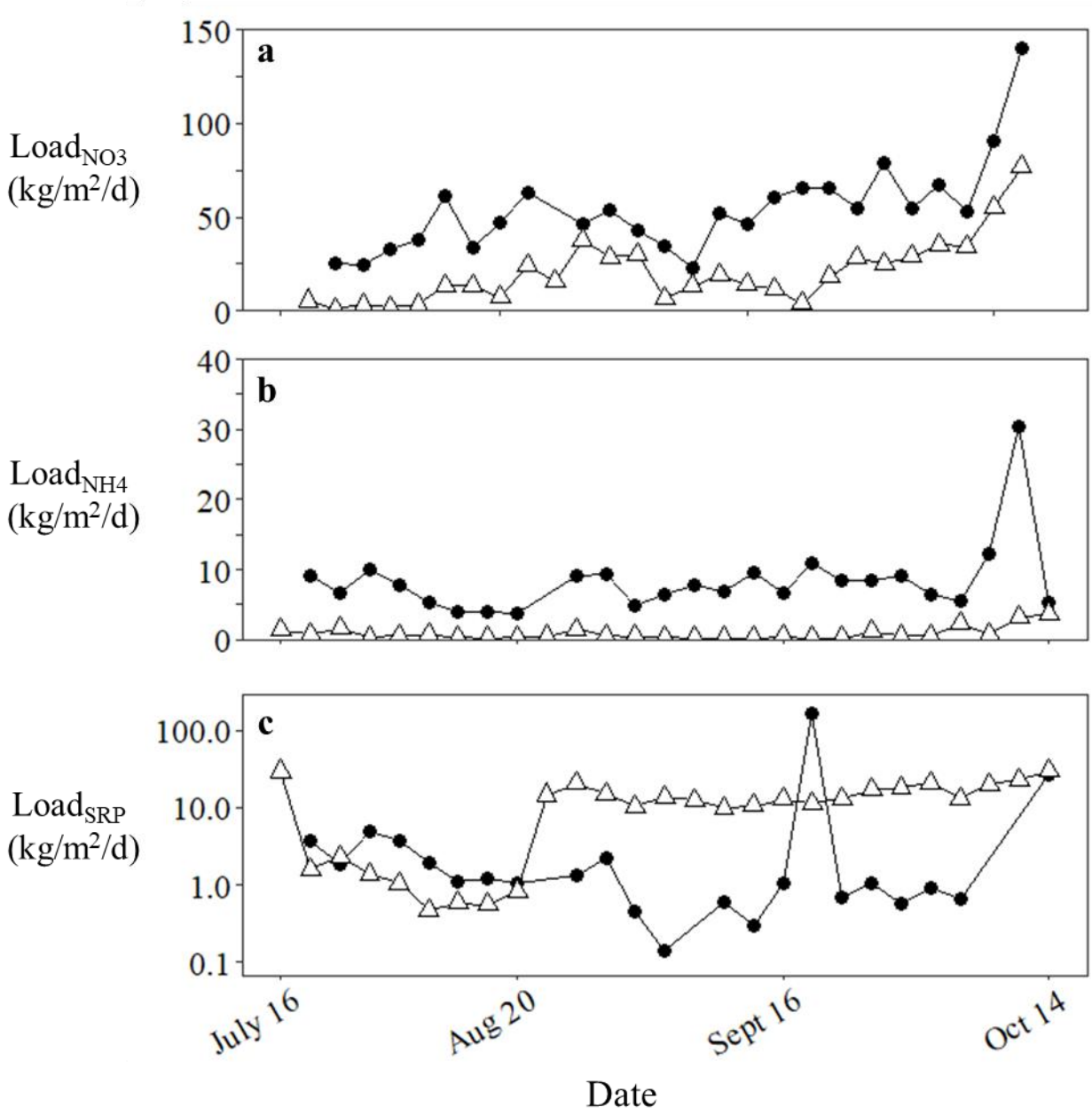

Figure S4: Trends in loads for (a) NO_3-N, (b) NH_4-N, and (c) SRP at Site 1 (closed cirlces) and 2 (open triangles).

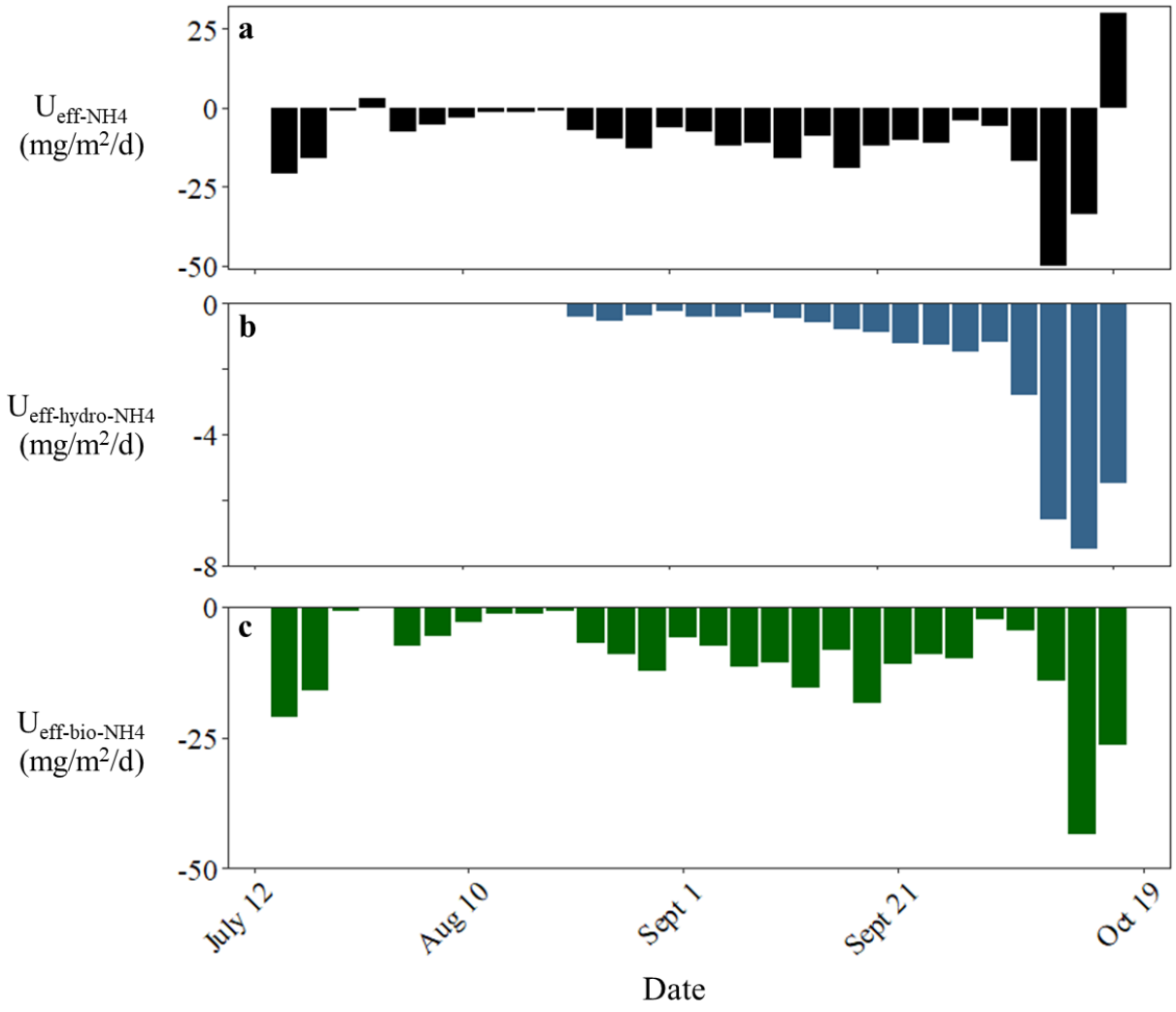

Figure S5: Temporal changes in (a) $U_{eff\text{-}NH4}$, (b) $U_{eff\text{-}hydro\text{-}NH4}$, and (c) $U_{eff\text{-}bio\text{-}NH4}$ derived from mass balance assessments at the reach scale over the course of the growing season. Lack of data for $U_{eff\text{-}hydro\text{-}NH4}$ prior to August 14 reflects net hydrologic gain contributing to increased downstream loads not measured during out study.

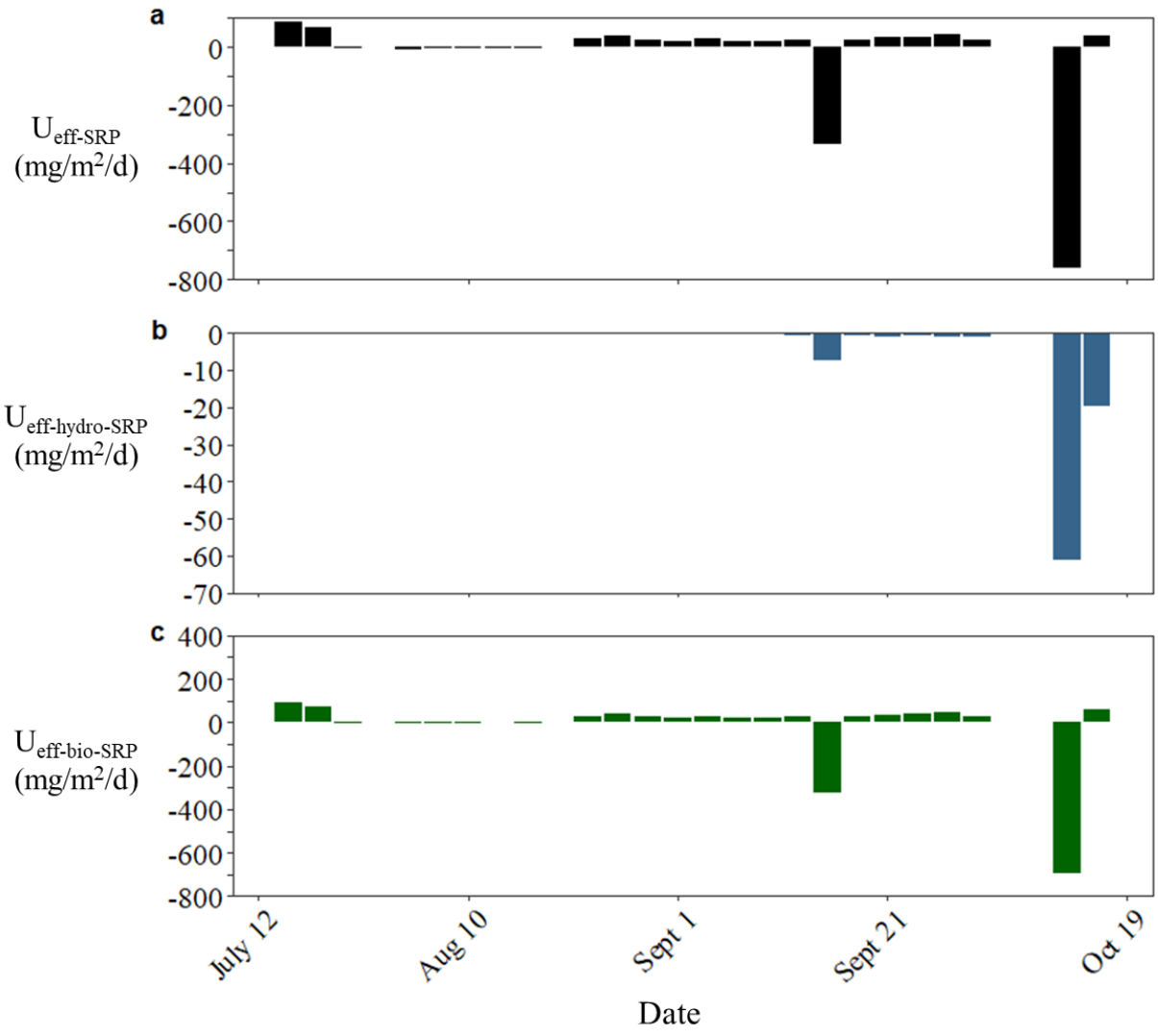

Figure S6: Temporal changes in (a) $U_{eff\text{-}SRP}$, (b) $U_{eff\text{-}hydro\text{-}SRP}$, and (c) $U_{eff\text{-}bio\text{-}SRP}$ derived from mass balance assessments at the reach scale over the course of the growing season. Lack of data for $U_{eff\text{-}hydro\text{-}NH4}$ prior to August 14 reflects net hydrologic gain contributing to increased downstream loads not measured during out study.

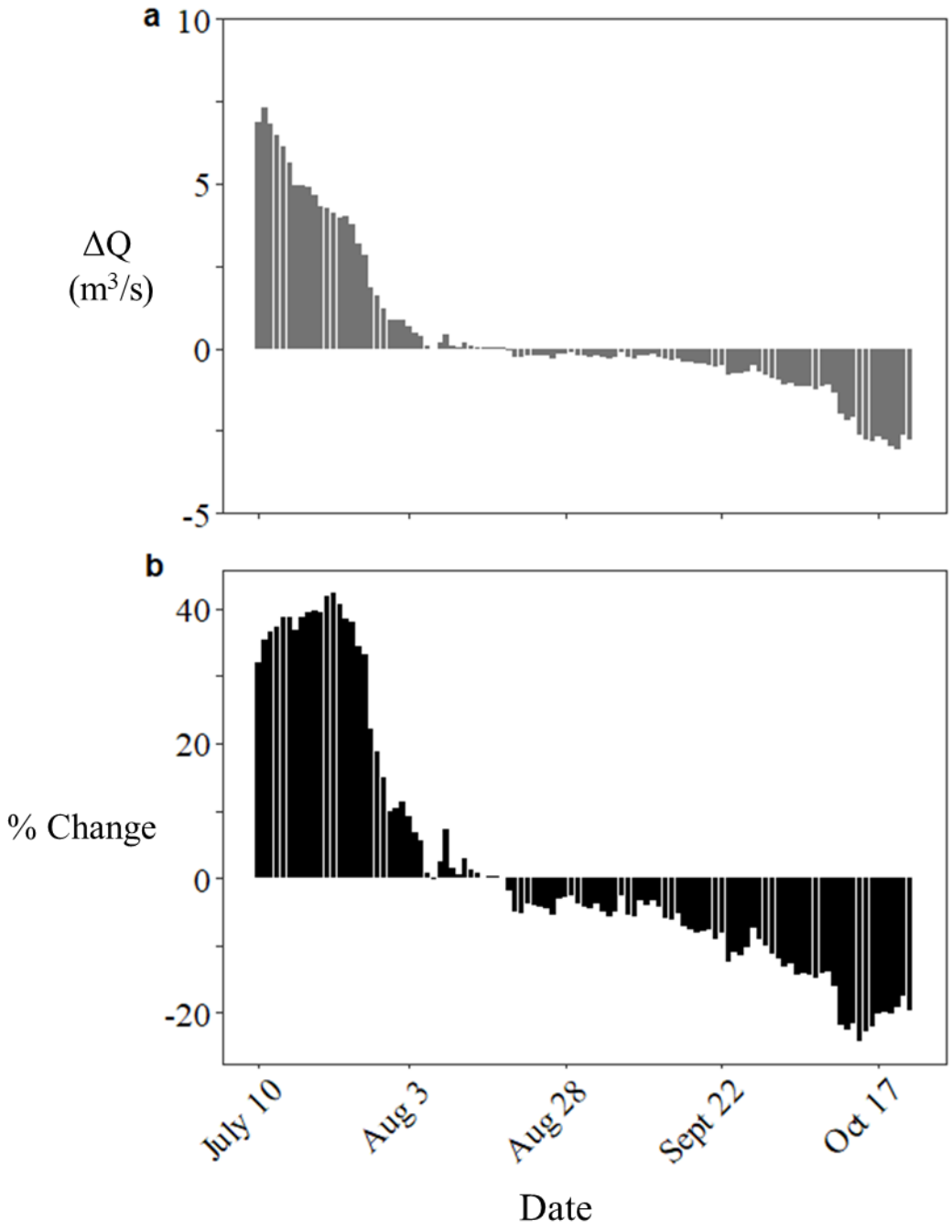

Figure S7: Trends in (a) absolute (m^3/s) and (b) percent change in discharge derived from differences in hydrologic load between the upstream and downstream sites.